

USARTL-TR-79-4

AD A069542

12



LEVEL

11

## HELICOPTER FLOW FIELD ANALYSIS

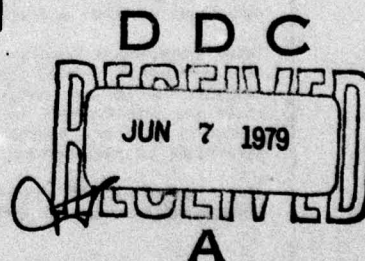
David R. Clark, Frank A. Dvorak, Brian Maskew  
J. Michael Summa, Frank A. Woodward  
Analytical Methods, Inc.  
100 - 116th Avenue S.E.  
Bellevue, Wash. 98004

April 1979

DDC FILE COPY

Final Report for Period April 1977 - September 1978

Approved for public release;  
distribution unlimited.



Prepared for

APPLIED TECHNOLOGY LABORATORY

U. S. ARMY RESEARCH AND TECHNOLOGY LABORATORIES (AVRADCOM)

Fort Eustis, Va. 23604

79 06 04 065

### APPLIED TECHNOLOGY LABORATORY POSITION STATEMENT

This report documents an engineering analysis and the resulting computer program which are considered to be technically sound for the prediction of helicopter fuselage flow fields without rotor wake effects. The computed results from the program should be used for design purposes only after correlation of the program with test data for an aircraft of similar configuration.

The computer program resulting from this contract will be provided to qualified users, upon request, for use in the design and analysis of rotary-wing aircraft.

The project engineer for this contract was Mr. W. D. Vann, Aeromechanics Technical Area, Aeronautical Technology Division.

Accession For	
NTIS Grant	<input checked="checked" type="checkbox"/>
DDC TAB	<input checked="checked" type="checkbox"/>
Unannounced	<input type="checkbox"/>
Justification	
By	
Institution/	
Availability Codes	
Dist	Avail and/or special
A	

#### DISCLAIMERS

The findings in this report are not to be construed as an official Department of the Army position unless so designated by other authorized documents.

When Government drawings, specifications, or other data are used for any purpose other than in connection with a definitely related Government procurement operation, the United States Government thereby incurs no responsibility nor any obligation whatsoever; and the fact that the Government may have formulated, furnished, or in any way supplied the said drawings, specifications, or other data is not to be regarded by implication or otherwise as in any manner licensing the holder or any other person or corporation, or conveying any rights or permission, to manufacture, use, or sell any patented invention that may in any way be related thereto.

Trade names cited in this report do not constitute an official endorsement or approval of the use of such commercial hardware or software.

#### DISPOSITION INSTRUCTIONS

Destroy this report when no longer needed. Do not return it to the originator.

Unclassified

SECURITY CLASSIFICATION OF THIS PAGE (When Data Entered)

REPORT DOCUMENTATION PAGE		READ INSTRUCTIONS BEFORE COMPLETING FORM	
1. REPORT NUMBER USARTI-TR-79-4	2. GOVT ACCESSION NO. TR-79-4	3. RECIPIENT'S CATALOG NUMBER	
4. TITLE (and Subtitle) HELICOPTER FLOW FIELD ANALYSIS	5. TYPE OF REPORT & PERIOD COVERED Final Report April 1977 - September 1978	6. PERFORMING ORG. REPORT NUMBER	
7. AUTHOR(s) David R. Clark, Frank A. Dvorak, Brian Maskew, J. Michael Summa, and Frank A. Woodward	8. CONTRACT OR GRANT NUMBER(s) DAAJ02-77-C-0028	9. PROGRAM ELEMENT, PROJECT, TASK AREA & WORK UNIT NUMBERS 62209A JEL26609AH76/00 195 EK	10. REPORT DATE April 1979
11. CONTROLLING OFFICE NAME AND ADDRESS Analytical Methods, Inc. 100 - 116th Avenue S.E. Bellevue, Washington 98004	12. NUMBER OF PAGES 79	13. SECURITY CLASS. (of this report) Unclassified	14. DECLASSIFICATION/DOWNGRADING SCHEDULE
15. MONITORING AGENCY NAME & ADDRESS (if different from Controlling Office) 80 p	16. DISTRIBUTION STATEMENT (of this Report) Approved for public release; distribution unlimited.	17. DISTRIBUTION STATEMENT (of the abstract entered in Block 20, if different from Report)	
18. SUPPLEMENTARY NOTES			
19. KEY WORDS (Continue on reverse side if necessary and identify by block number) Drag, Helicopters, Bodies, Wings, Potential Flow, Streamlines, Boundary Layer, Viscous Flow, Separated Flow, Configuration Modeling			
20. ABSTRACT (Continue on reverse side if necessary and identify by block number) A computer program has been developed which allows the flow around general aircraft configurations to be modeled, including the effects of regions of separated flow. The program, although developed specifically to handle the regions of separated flow associated with the typically bluff helicopter airframes, retains the capability to model the more slender shapes associated with fixed-wing aircraft. The flow around the specified configu- ration is calculated iteratively, the first step being the solution of the			

DD FORM 1 JAN 73 1473 EDITION OF 1 NOV 65 IS OBSOLETE

Unclassified

SECURITY CLASSIFICATION OF THIS PAGE (When Data Entered)

392 078

alt

Unclassified

SECURITY CLASSIFICATION OF THIS PAGE(When Data Entered)

basic potential flow. This is followed by the definition of the potential flow streamlines over the surface, the calculation of boundary layer growth along the streamlines, the identification of the separated flow region and the eventual recalculation of the potential flow, including the effects of boundary layer growth and separated flow. The iterations between potential and viscous flow may be repeated as often as desired. During its development, the program has been exercised on a number of helicopter and aircraft configurations. This experience has shown that the program can be used to model the flow about the involved shapes typical of the new generation of rotorcraft now going into service without any increase in difficulty, either in preparing the input data or in executing the solution, when compared with earlier purely potential flow solutions. ↗

Unclassified

SECURITY CLASSIFICATION OF THIS PAGE(When Data Entered)

### PREFACE

This program was sponsored by the Applied Technology Laboratory, U.S. Army Research and Technology Laboratories (AVRADCOM), Fort Eustis, Virginia, and was carried out under Contract DAAJ02-77-C-0028. The contract monitor was Mr. W.D. Vann, and the authors would like to take this opportunity to acknowledge his helpful comments and constructive criticism during the course of the study.

## TABLE OF CONTENTS

<u>Section</u>	<u>Page</u>
PREFACE . . . . .	3
LIST OF ILLUSTRATIONS . . . . .	6
INTRODUCTION . . . . .	7
GEOMETRY DEFINITION . . . . .	9
POTENTIAL FLOW MODEL . . . . .	12
Aerodynamic Representation . . . . .	18
Potential Flow Solution . . . . .	19
STREAMLINE CALCULATION . . . . .	22
Computation of the Partial Derivatives . . . . .	22
Computation of Points on a Streamline . . . . .	24
Search Routine . . . . .	29
WIND TUNNEL . . . . .	31
ENGINE INLET/EXHAUST REPRESENTATION . . . . .	33
APPLICATIONS . . . . .	35
CONCLUSIONS AND RECOMMENDATIONS . . . . .	52
REFERENCES . . . . .	53
APPENDIX A. Program User's Guide . . . . .	54

# LIST OF ILLUSTRATIONS

<u>Figure</u>		<u>Page</u>
1	Patch Representation of Body Geometry . . . . .	10
2	Patch Joint Schematic . . . . .	11
3	Panel Model of Typical Utility Transport Helicopter . . . . .	36
4	Panel Model of Typical Attack Helicopter . . . . .	37
5	Partial Attack Helicopter Model on Wind Tunnel Ground Plane . . . . .	39
6	UH-60A Pressure Distribution Along Top Centerline . . . . .	41
7	YAH-64 Pressure Distribution Along Top Centerline . . . . .	42
8	Pressure Distribution Above Ground Plane on Transport Helicopter Model . . . . .	43
9	Pressure Distribution Around a Body Station Cut on Transport Helicopter Model . . . . .	44
10	Pressure Distribution Around Buttline Cut on Attack Helicopter Model . . . . .	45
11	Streamline Trajectories on Side of Attack Helicopter Fuselage . . . . .	46
12	Navy/ARPA Lockheed X-Wing Front View Without Wings . . . . .	47
13	Navy/ARPA Lockheed X-Wing Full Configuration . . . . .	48
14	X-Wing Pressure Distributions Along Tip and Bottom Centerlines . . . . .	50
15	Pressure Distributions on Wings at 29% Span . . . . .	51

## INTRODUCTION

Until very recently, design for low drag has never been a major constraint in the development of rotary wing aircraft since with cruise speeds never much more than 100 knots, the contribution of the airframe to the total power consumed has been relatively minor when compared with the rotor effects. However, with the cruise requirement raised to 145 knots, as it has been for both the Armed Attack Helicopter (AAH) and the Utility Tactical Transport Aircraft System (UTTAS), airframe drag is playing a more significant part. This, together with configuration design constraints introduced by other factors (such as air transportability) and the need to define achievable performance relative to a very challenging specification, underscored the need for a reliable means of predicting drag during the design process.

Traditional empirical drag estimation methods are notoriously imprecise, even when used within a given generation of rotorcraft, and when used to evaluate a design where there is a jump in the level of technology, they cannot be expected to be reliable. Where the configuration is slender, such as most fixed wing aircraft in the cruise configuration, and where there are no regions of separated flow, potential flow solutions and a subsequent boundary layer and skin friction calculation provide a good estimate of drag. Unfortunately, on the typical helicopter configuration bluff shapes are the rule rather than the exception, regions of separated flow are present on most of the aft-facing surfaces, and potential flow methods are inadequate. It was to provide a method by which paneling methods developed for potential flow field modeling could be extended to the bluff body helicopter problem that the work described in Reference 1 was carried out.

In the study described in Reference 1, a potential flow method in which the body was represented by a number of flat source panels was used as the basis for a streamline and boundary layer calculation. Separation location was identified on each streamline, and with the presence of the boundary layer thickness and separated flow region modeled, the calculation was recycled through the flow field calculation. This process was repeated as often as was needed to converge on a solution.

The computer program, code named DRAG, demonstrated the ability to predict as part of the aerodynamic calculation the base pressure in separated flow regions. The program was deficient in two areas, however. First, in order to take advantage of an existing streamline tracing procedure, each column of panels was constrained to have the same number of rows. This assumption of a regular panel grid resulted in considerable reduction of streamline computation effort, but made the task of paneling the configuration somewhat more difficult, the user being restricted to simple, regular bodies, or if

- 
1. Dvorak, F.A., Maskew, B., and Woodward, F.A., "Investigation of Three-Dimensional Flow Separation on Fuselage Configurations", USAAMRDL-TR-77-4, Eustis Directorate, U.S. Army Air Mobility R & D Laboratory, Fort Eustis, Virginia, March 1977, AD A039382.

complex bodies were required, to inefficient panel densities in some regions of the body.

Second, close to the separation point, there existed a sharp excursion in the calculated pressures which was absent in the experimental data. The reason for the anomaly lies in the type of singularity chosen to model the body. In this case, carrying over from an earlier model, constant source panels were used on the body surface, while the separated wake was represented by constant vorticity panels. Consequently, an abrupt change in both singularity type and strength was introduced.

The present study was undertaken to remove the constraints existing in the DRAG program. As part of this effort, several improvements and additional capabilities were provided for the user of the program. The patching/paneling restriction was removed by going to a multi-patch representation of the body, retaining within each patch the regular structure required by program DRAG while requiring only the patch joint information in addition to the basic input. This provides a very efficient and flexible paneling scheme. The irregularity in the pressures calculated was removed by going to a higher-order singularity in place of the simple constant strength sources used in the original code. Additional features added include the ability to model wind tunnel walls and floor, and engine efflux modeling.

The program in its present form has been used to model the flow about representative helicopter configurations, and examples of its use are presented in the report.

### GEOMETRY DEFINITION

As in the original version of the DRAG program, a configuration is represented geometrically by a network of interconnected panels. Within the program there are a number of routines which require information from neighboring panels (e.g., streamline tracing, boundary layer source and skin friction redistribution, surface vorticity continuity). This information is readily available from a rectangular grid of panels as used in the basic version of the DRAG program. A single rectangular grid, however, is very restrictive for applications to practical problems and so a scheme has been developed based on multiple PATCHES of panels (Figure 1). Each patch has a rectangular grid of panels and so maintains the ease of obtaining neighboring panel information within itself. A special SEARCH routine (described in a later section) has been developed to determine information on neighboring panels across the patch edges where there is not necessarily a direct correlation between neighboring panels. Each patch, therefore, is a complete unit in the sense that its panel spacing is not necessarily related to a neighboring patch. In this way, very general configurations can be paneled. Clearly, however, the number of patches should be kept as small as possible, consistent with reasonable panel shapes. Patch surfaces (when opened out) should be usually four-sided, although one side or two opposite sides can degenerate to points, producing triangular panels locally.

The patches are numbered automatically by the program as it constructs the panel model in WBPANX, the patch number being a function of the order in which the section input is read. The key parameter in determining patching is the parameter, Flag, on Card 10B of the input deck. When a value of 1 is read for this parameter, the code knows that the last section of a patch is being read. It then assigns a patch number to the panels constructed since the last section, read with FLAG = 1, records the number of rows and columns in the patch and the number of the last panel in the patch. This information is used in the solution of the influence coefficient matrix in the streamline calculation.

The number (order) of the patches may be deduced from the input data deck and has to be known in order to supply the streamline code with information on neighboring panels. This is supplied in the form of a table of patch side overlaps, the patch sides being numbered anti-clockwise when viewed from outside the body with side one being that side closest to the front of the body. A typical patch schematic

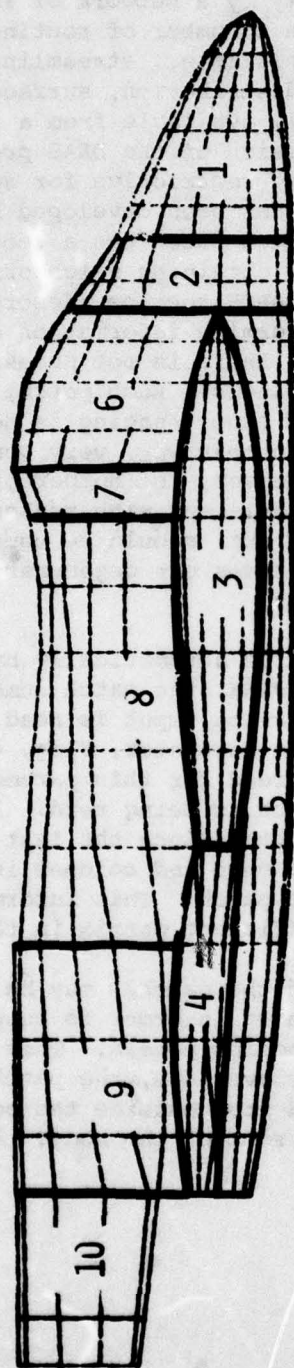


Figure 1. Patch Representation of Body Geometry.

for the body shown in Figure 1 is given in Figure 2. A partial list of the patch joint information is given below.

PATCH	SIDE	OVERLAPS	PATCH	SIDE
1	3	"	2	1
1	4	"	1	4
1	2	"	1	2
2	4	"	2	2
2	2	"	2	2
2	3	"	5	1
2	3	"	3	1
2	3	"	6	1

Since the body is symmetric, the joint along the middle of the model is a reflection with the patch being overlapped by itself (on the other side). Hence 1,4 overlaps 1,4. Also, even though side 1 of patch 3 is a point (actually two points superimposed), it must be modeled if passage of a streamline through that region is desired.

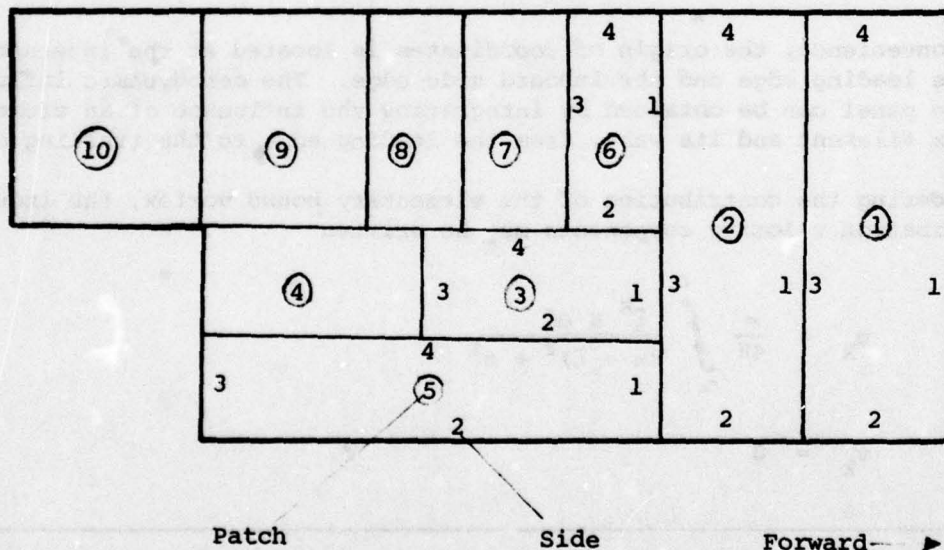
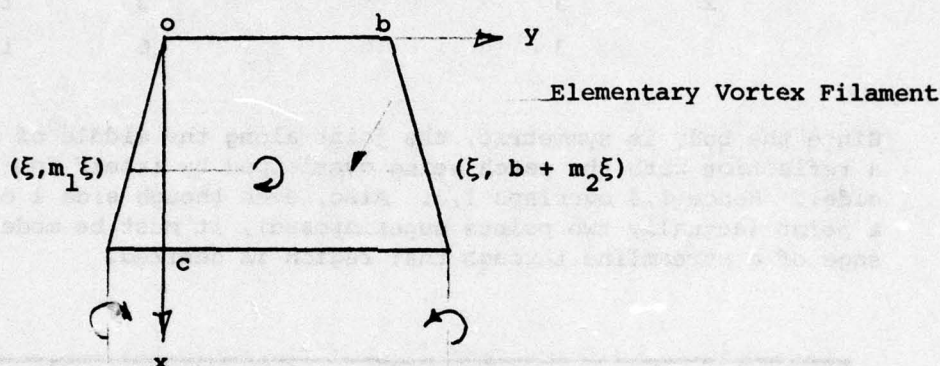


Figure 2. Patch Joint Schematic.

### POTENTIAL FLOW MODEL

A new potential flow model has been developed to replace the original constant source panel representation described in Reference 2. The new aerodynamic singularity consists of a combination of constant and linearly varying vortex distributions on the body panels. This type of singularity has been successfully applied to the analysis of separated flows on two-dimensional airfoils (Ref. 3). A generalization of these vortex singularities suitable for the analysis of arbitrary body shapes is derived below.

Consider a typical body panel having unswept leading and trailing edges, arbitrary edge slopes,  $m_1$  and  $m_2$ , and chord length,  $c$ .



For convenience, the origin of coordinates is located at the intersection of the leading edge and the inboard side edge. The aerodynamic influence of the panel can be obtained by integrating the influence of an elementary vortex filament and its wake, from the leading edge to the trailing edge.

Considering the contribution of the elementary bound vortex, the induced perturbation velocity components may be written

$$u_k = \frac{z}{4\pi} \int_0^c \frac{\xi^k K d\xi}{(x - \xi)^2 + z^2} \quad (1)$$

$$v_k = 0 \quad (2)$$

2. Woodward, F.A., Dvorak, F.A., and Geller, E.W., "A Computer Program for Three-Dimensional Lifting Bodies in Subsonic Inviscid Flow", USAAMRDL TR-74-18, Eustis Directorate, U.S. Army Air Mobility Research and Development Laboratory, Fort Eustis, Va., April 1974, AD 782202.
3. Maskew, B., and Dvorak, F.A., "The Prediction of  $C_{l_{max}}$  Using a Separated Flow Model", J. Am. Hel. Soc., April 1978.

$$w_k = \frac{-1}{4\pi} \int_0^c \frac{(x - \xi) \xi^k K d\xi}{(x - \xi)^2 + z^2} \quad (3)$$

where

$$K = \frac{y - m_1 \xi}{\sqrt{(x - \xi)^2 + (y - m_1 \xi)^2 + z^2}} - \frac{y - b + m_2 \xi}{\sqrt{(x - \xi)^2 + (y - b - m_2 \xi)^2 + z^2}}$$

and  $k = 0$  for constant vortex distribution, and  
 $k = 1$  for linearly varying vortex distribution.

Similarly, the contribution of the elementary vortex along a panel side edge of slope,  $m$ , may be written

$$\bar{u}_{k+1} = -m \bar{v}_{k+1} \quad (4)$$

$$\bar{v}_{k+1} = \frac{-z}{4\pi r^2} \int_0^c \xi^k K_E d\xi \quad (5)$$

$$\bar{w}_{k+1} = \frac{y - mx}{4\pi r^2} \int_0^c \xi^k K_E d\xi \quad (6)$$

where  $K_E = \frac{x + my - (1 + m^2)\xi}{\sqrt{(x - \xi)^2 + (y - m - \xi)^2 + z^2}}$

$$- \frac{x - c + m(y - mc)}{\sqrt{(x - c)^2 + (y - mc)^2 + z^2}}$$

$$r^2 = (mx - y)^2 + (1 + m^2)z^2$$

and  $k = 0$  for linear edge vortex associated with constant vortex distribution, and

$k = 1$  for quadratic edge vortex associated with linear vortex distribution.

Evaluating the above integrals, the following results are obtained for the three components of velocity at a point  $(x, y, z)$  induced by the bound vortex distributions.

#### Constant Bound Vortex Distribution

$$u_o = \frac{F}{4\pi} \quad (7)$$

$$v_o = 0 \quad (8)$$

$$w_o = -\frac{1}{4\pi} (mG - H) \quad (9)$$

### Linear Bound Vortex Distribution

$$u_1 = \frac{1}{4\pi c} \left[ xF - z(mG - H) \right] \quad (10)$$

$$v_1 = 0 \quad (11)$$

$$w_1 = \frac{-1}{4\pi c} \left[ x(mG - H) + zF - \frac{1}{1+m^2} \left( (y - mx) G + mD \right) \right] \quad (12)$$

where  $D = \sqrt{x^2 + y^2 + z^2}$

$$F = \tan^{-1} \frac{zD}{x(mx - y) + mz^2}$$

$$G = \frac{1}{\sqrt{1+m^2}} \sin h^{-1} \frac{x + my}{r}$$

$$H = \sin h^{-1} \frac{y}{\sqrt{x^2 + z^2}}$$

These expressions give the influence of a single corner of the panel, with the origin of coordinates located at that corner. The influence of the complete panel is obtained by summing the influences of each of the four corners.

The contribution of an edge vortex is given by the following expressions:

Constant Edge Vortex

$$\bar{u}_0 = -mz v_c \quad (13)$$

$$\bar{v}_0 = z.v \quad (14)$$

$$\bar{w}_0 = (mx - y) v_c \quad (15)$$

Linear Edge Vortex

$$\bar{u}_1 = -mzV_L \quad (16)$$

$$\bar{v}_1 = zV_L \quad (17)$$

$$\bar{w}_1 = (mx - y) V_L \quad (18)$$

Quadratic Edge Vortex

$$\bar{u}_2 = -mzV_Q \quad (19)$$

$$\bar{v}_2 = zV_Q \quad (20)$$

$$\bar{w}_2 = (mx - y) V_Q \quad (21)$$

where 
$$v_c = \frac{1}{4\pi r^2} \left( \frac{x + my}{D} - \frac{x - c + m(y - mc)}{D_T} \right)$$

$$v_L = \frac{1}{4\pi r^2} \left( D - D_T - \frac{c(x - c + m(m - mc))}{D_T} \right)$$

$$v_Q = \frac{1}{8\pi} \left\{ \frac{1}{r^2} \left[ \frac{(x + my)D - (x - c + m(y - mc))D_T}{(1 + m^2)} - 2c D_T \right. \right. \\ \left. \left. - c^2 \frac{(x - c + m(y - mc))}{D_T} \right] + \frac{G - G_T}{1 + m^2} \right\}$$

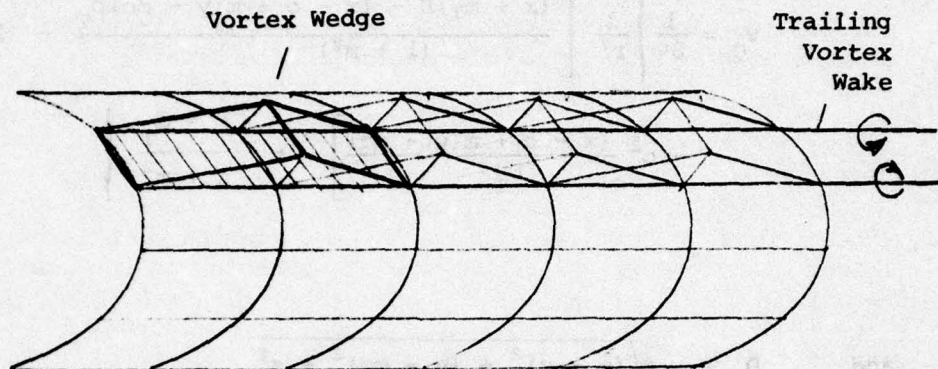
and 
$$D_T = \sqrt{(x - c)^2 + (y - mc)^2 + z^2}$$

$$G_T = \frac{1}{\sqrt{1 + m^2}} \sinh^{-1} \frac{x - c + m(y - mc)}{r}$$



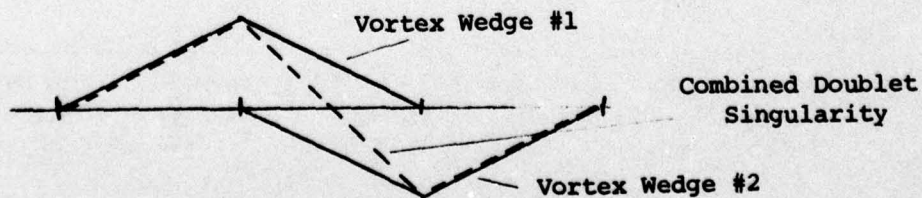
## AERODYNAMIC REPRESENTATION

The body surface is subdivided into a number of patches, each patch having a fixed number of rows and columns. Within each patch, the constant and linearly varying vortex singularities are formed into overlapping wedges over pairs of adjacent panels along each column, as illustrated below.



The aerodynamic influence of each vortex wedge includes the contributions of the constant and linearly varying bound vorticity, the edge vorticity, and a pair of concentrated vortices trailing downstream in the wake. The unknown vortex strength is the height of the wedge, while the control points (used for satisfying the boundary conditions of tangential flow) are located at panel centroids.

For convenience in accounting for the influence of the vortex wake, adjacent pairs of vortex wedges are combined to form doublets. The strengths of the vortex wedges are weighted according to the chord lengths of the panels such that the trailing vortices from each wedge exactly cancel in the wake. The resulting doublet singularity extends over three adjacent panels as shown below. The control point is located at the centroid of the middle panel.



In the application of the doublet singularity, special care is required at the junction of two patches to ensure conservation of vorticity. The last two rows on the upstream patch contain truncated doublet singularities. Vorticity is conserved within this patch by introducing stepwise constant line vortices along the trailing edge of the patch. The strengths of these edge vortices are proportional to that of the corresponding truncated doublet. This concentrated trailing-edge vorticity is then transferred to the leading edge of the downstream patch. This in turn is fed into the nearest side edges of the first row of panels in this patch and distributed linearly over each of these panels. In this way any residual vorticity can be exactly cancelled by the first row of panels. The influence of the remaining doublet singularities in the downstream patch can then be computed in the usual way.

#### POTENTIAL FLOW SOLUTION

The doublet singularities are used to calculate the normal velocity at panel control points, resulting in the formation of a large system of linear equations relating the doublet strengths to the prescribed normal velocity of each control point. However, the use of doublet singularities alone is not sufficient to ensure a unique solution. A constant source singularity is also distributed over each panel and used to calculate the normal velocity at the control points around the first ring of panels at the body nose. The resulting system of equations may then be solved to determine the unknown source and doublet strengths.

The numerical stability of this system of equations can be improved by introducing additional constant source singularities on each panel. The strengths of these additional sources are set equal to the axial component of the onset flow. For onset flows parallel to the x-axis, this is equivalent to applying the Green's Identity formulation described in Reference 4. This additional source distribution has the effect of reducing the doublet strengths required to satisfy the boundary condition equations, and significantly improves the numerical stability and convergence of the solution:

The resulting system of equations may be written in matrix form as follows:

$$A_{ij} \gamma_j = B_{ij} \sigma_j + N_i \quad (22)$$

- 
4. Bristow, D.R., and Grose, G.G., "Modification of the Douglas Neumann Program to Improve the Efficiency of Predicting Component Interference and High Lift Characteristics," NASA CR-3020, January 1978.

where  $A_{ij} = n_{x_i} \cdot u_{D_{ij}} + n_{y_i} \cdot v_{D_{ij}} + n_{z_i} \cdot w_{D_{ij}}$

$$B_{ij} = n_{x_i} \cdot u_{s_{ij}} + n_{y_i} \cdot v_{s_{ij}} + n_{z_i} \cdot w_{s_{ij}}$$

$$N_i = n_{x_i} \cdot \cos \alpha \cos \beta + n_{y_i} \cdot \sin \beta + n_{z_i} \cdot \sin \alpha \cos \beta;$$

$$\sigma_j = n_{x_j} / 4\pi = \text{prescribed source strength};$$

$$\gamma_j = \text{unknown doublet strength};$$

and  $n_{x_i}, n_{y_i}, n_{z_i} = \text{direction cosines of normal to control point of panel, } i;$

$$u_{D_{ij}}, v_{D_{ij}}, w_{D_{ij}} = \text{three components of velocity induced by source, } j, \text{ on control point, } i; \text{ and}$$

$$\alpha, \beta = \text{angles of attack and yaw of onset flow.}$$

Once the doublet strengths have been determined, the three components of velocity at control point,  $i$ , can be computed as follows:

$$u_i = u_{D_{ij}} \gamma_j + u_{s_{ij}} \sigma_j + \cos \alpha \cos \beta \quad (23)$$

$$v_i = v_{D_{ij}} \gamma_j + v_{s_{ij}} \sigma_j + \sin \beta \quad (24)$$

$$w_i = w_{D_{ij}} \gamma_j + w_{s_{ij}} \sigma_j + \sin \alpha \cos \beta \quad (25)$$

The pressure coefficient in incompressible flow is then given by

$$C_{p_i} = 1 - u_i^2 - v_i^2 - w_i^2 \quad (26)$$

The calculation of the forces and moments on the body is given by Equations (28) through (32) of Reference 2.

#### COMPUTATION OF THE INITIAL DERIVATIVES

The gradients of the velocity components and the force components are shown on the following sketch. The gradients of the velocity components are indicated by the letters U, V, W, X, Y, Z, and the force components by F, G, H, I, J, K, L, M, N, O, P, Q, R, S, T, U, V, W, X, Y, Z.



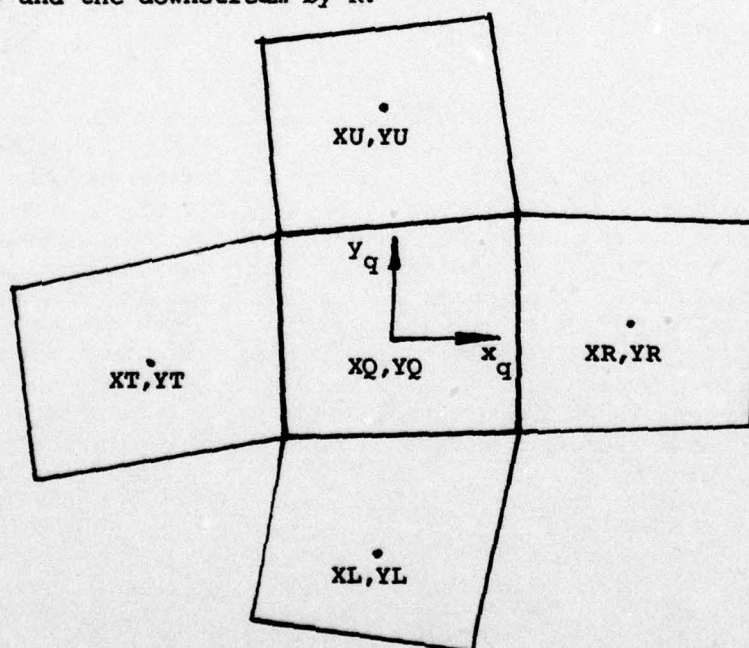
U. S. Navy, C. W. 1. A. 1. The Calculation of Gradients Data for Boundary Layer Flow. NND-6-10. January 1966.

### STREAMLINE CALCULATION

The DRAG program computes an approximate solution to the problem of three-dimensional potential flow over an arbitrary body. As described earlier, the body surface is now represented by a set of patches. Within each patch a set of plane quadrilaterals are arranged in a rectangular grid; however, the grid of panels can vary from one patch to another. The three components of the velocity vector are computed at the panel centroids. The streamline program uses the velocity data at four neighboring panels to provide a linear approximation to the velocity anywhere on a given panel. A straight-line approximation to the actual streamline passing through a point on the panel is constructed and continued over all panels upstream and downstream. This results in relatively smooth streamlines over the body, and allows the geodesic curvatures of the streamlines and equipotential lines to be computed. From this information, the metric or effective radius of the body along the streamline is obtained. The method used follows closely that described in Reference 5.

### COMPUTATION OF THE PARTIAL DERIVATIVES

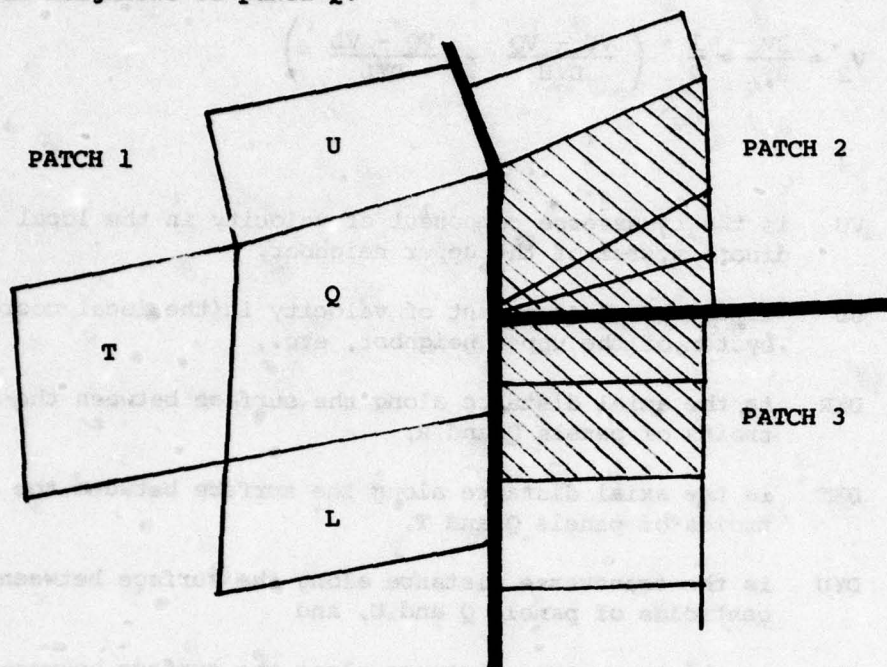
The quadrilateral under consideration and its four neighbors are shown on the following sketch. The quadrilateral coordinate system is identified by the letter Q, the upper neighbor by U, the lower by L, the upstream by T, and the downstream by R.



---

5. Dawson, C.W., and Dean, J.S., "The Calculation of Streamline Data for Boundary Layer Input", NSRDC CMD-4-74, January 1974.

If panel Q borders on a patch edge, then SEARCH is called, and an array identifying all panels adjacent to the panel edge is generated. In the example sketched below, the "shaded" panels would be listed as downstream neighbors of panel Q.



Initially, any one of these panels is selected as the downstream neighbor, R, depending on the order of description of the joints between the participating patches. Ultimately, neighbor R is selected by requiring that the predicted intersection point be adjacent to the panel edge. This procedure is explained in more detail in the section describing SEARCH. The new streamline code also ensures that the existing panel (previous panel Q) is employed as a neighbor to panel Q. Once the neighbors are identified, the neighboring panels are assumed to be rotated about the common edges so that all panels lie in the same plane as the central quadrilateral. The program then computes the velocity and position vectors of the neighbors in terms of the central panel coordinate system. From this construction, the following partial derivatives are obtained:

$$u_1 = \frac{\partial U}{\partial x_q} = \frac{1}{2} \left( \frac{UR - UQ}{DXR} + \frac{UQ - UT}{DXT} \right) \quad (27)$$

$$u_2 = \frac{\partial U}{\partial y_q} = \frac{1}{2} \left( \frac{UU - UQ}{DYU} + \frac{UQ - UL}{DYL} \right) \quad (28)$$

$$v_1 = \frac{\partial v}{\partial x_q} = \frac{1}{2} \left( \frac{v_R - v_Q}{DXR} + \frac{v_Q - v_T}{DXT} \right) \quad (29)$$

$$v_2 = \frac{\partial v}{\partial y_q} = \frac{1}{2} \left( \frac{v_U - v_Q}{DYU} + \frac{v_Q - v_L}{DYL} \right) \quad (30)$$

where  $VU$  is the transverse component of velocity in the local coordinate system of the upper neighbor,

$UU$  is the axial component of velocity in the local coordinate system of the upper neighbor, etc.,

$DXR$  is the axial distance along the surface between the centroids of panels  $Q$  and  $R$ ,

$DXT$  is the axial distance along the surface between the centroids of panels  $Q$  and  $T$ ,

$DYU$  is the transverse distance along the surface between the centroids of panels  $Q$  and  $U$ , and

$DYL$  is the transverse distance along the surface between the centroids of panels  $Q$  and  $L$ .

The axial and transverse components of velocity on panel  $Q$  are then approximately

$$U = U_q + U_1 x_q + U_2 y_q \quad V = V_q + V_1 x_q + V_2 y_q \quad (31)$$

#### COMPUTATION OF POINTS ON A STREAMLINE

The streamline computation begins at a given point in a specified quadrilateral with the velocity vector,  $V = (U, V)$ . A stream function is desired which will have a constant value of zero along the streamline. Since the divergence of  $\vec{V}$  is not zero, an additional function,  $\rho$ , must be found such that the divergence of  $\rho V$  is zero. Then for a particle following a streamline,

$$\frac{dy}{dx} = \frac{dy/dt}{dx/dt} = \frac{V}{U} = \frac{\rho V}{\rho U} \quad (32)$$

Thus, a new vector field is constructed whose streamlines are identical to those of the velocity field, but whose divergence is zero. The function,  $\rho$ , is given by the series

$$\rho(x_q, y_q) = 1 - \frac{U_q (U_1 + V_2)}{U_q^2 + V_q^2} x_q - \frac{V_q (U_1 + V_2)}{U_q^2 + V_q^2} y_q + \dots \quad (33)$$

The resulting stream function is

$$\begin{aligned} SF(x_q, y_q) = SF_0 - V_q x_q + U_q y_q - & \left[ V_1 - \frac{U_q V_q (U_1 + V_2)}{U_q^2 + V_q^2} \right] \frac{x_q^2}{2} \\ & + \left[ U_2 - \frac{U_q V_q (U_1 + V_2)}{U_q^2 + V_q^2} \right] \frac{y_q^2}{2} \\ & + \left[ U_1 - \frac{U_q^2 (U_1 + V_2)}{U_q^2 + V_q^2} \right] x_q y_q + \dots \quad (34) \end{aligned}$$

The constant value,  $SF_0$ , is chosen so that the stream function is zero at the specified point. Since the velocity is known only through the linear terms, it is consistent to truncate the stream function after the quadratic terms.

Values of SF at the four corner points of the quadrilateral are now computed. By comparing the signs of SF at adjacent corners, the sides through which the streamline passes are determined. If the streamline passes through a side, the value of SF is computed at the midpoint of the side. From these three points, the intersection point is computed from a three-point interpolation formula.

The parameter,  $t(0 \leq t \leq 1)$ , is defined so that

$$\begin{aligned} x &= x_1 + t(x_3 - x_1) \\ y &= y_1 + t(y_3 - y_1) \end{aligned} \quad (35)$$

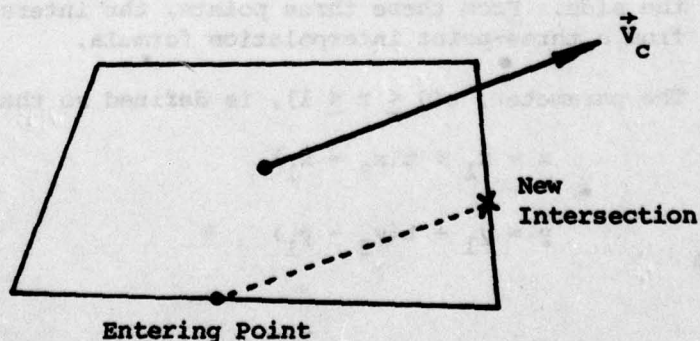
Here,  $x, y$  is the intersection point,  
 $x_1, y_1$  is one corner point,  
 $x_3, y_3$  is the other corner point, and  
 $x_2, y_2$  is the middle point.

Then,

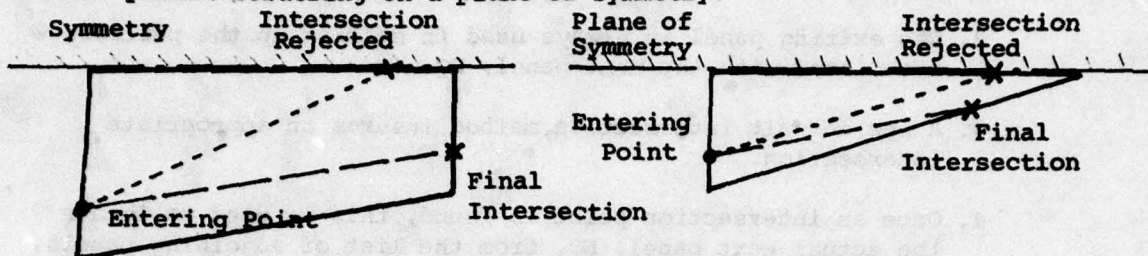
$$0 = SF(x, y) = 2SF_1(t - \frac{1}{2})(t - 1) - 4SF_2t(t - 1) + 2SF_3t(t - \frac{1}{2}) \quad (36)$$

The root of this equation is chosen so that  $0 \leq t \leq 1$ . Note that if there had been two roots between 0 and 1, then SF would have the same sign at both corner points, and those intersection points would be ignored.

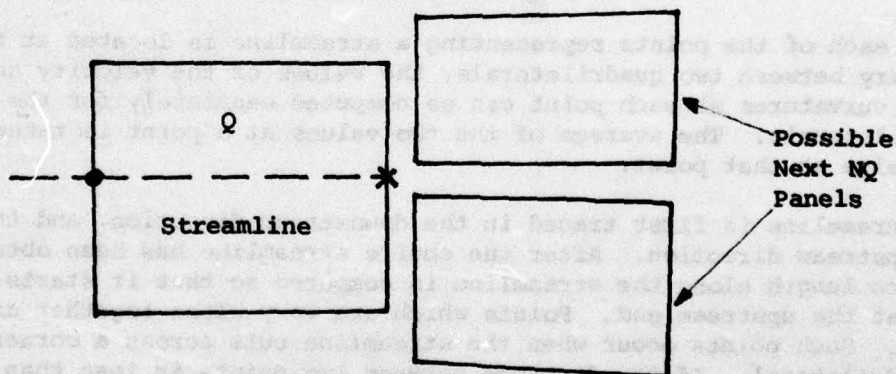
In general, two intersections will be found for the entire quadrilateral: one where the streamline enters, and one where it leaves. It is possible, however, for there to be four intersection points. The next point on the streamline is chosen from the intersection points as follows: a quantity, TESTP, is computed for each intersection point by taking the dot product of the vector from the starting point to the intersection point with the velocity vector at the centroid of the quadrilateral, and then multiplying it by the direction sign. (The direction sign is +1 if the streamline is being traced upstream.) The intersection point with the maximum positive value of TESTP is chosen. However, if the largest TESTP is less than or equal to zero, none of the points is acceptable. In general, this will occur in places where the panel spacing changes abruptly across patch edges and/or where the actual body curvature changes abruptly. In these cases, the approximations outlined above in calculating the partial derivatives can become too large; consequently, to continue the streamline, the fluid particle is assumed to travel across the panel from the entering point at a velocity equal to the velocity at the panel centroid as indicated in the following sketch.



Panels bordering on a plane of symmetry sometimes require special handling. If the calculated intersection point lies on the plane of symmetry, this point is rejected and the final intersection point is calculated geometrically on the upstream or downstream edge of finite length, depending on the direction of the streamline calculation. The sketch below illustrates resultant streamline shapes across two different panels bordering on a plane of symmetry.



If the current panel borders on a patch edge and the streamline is to cross onto the next patch, then the final intersection point is used to select the next panel from the list of adjoining panels discussed earlier. Because there are generally small gaps between the panels, this selection process must be carefully done to ensure continuation of the streamline calculation. For example, intersection points that lie in an interstice require special handling (see sketch below).



Here, an entering point very close to the corner point of each possible next panel,  $NQ$ , is assumed in turn and the streamline procedure continues. If the stream function values on the new panel indicate a good future intersection, then that particular panel is chosen as the neighbor to panel  $Q$  in the sketch above. A final check is made in all cases to assure that the final next panel,  $NQ$ , has actually participated in the calculation of the partial derivatives associated with the streamline

crossing of panel Q. If not, the crossing of panel Q is repeated with NQ used as the appropriate neighbor.

In summary, the new features provided in STREAM are the following:

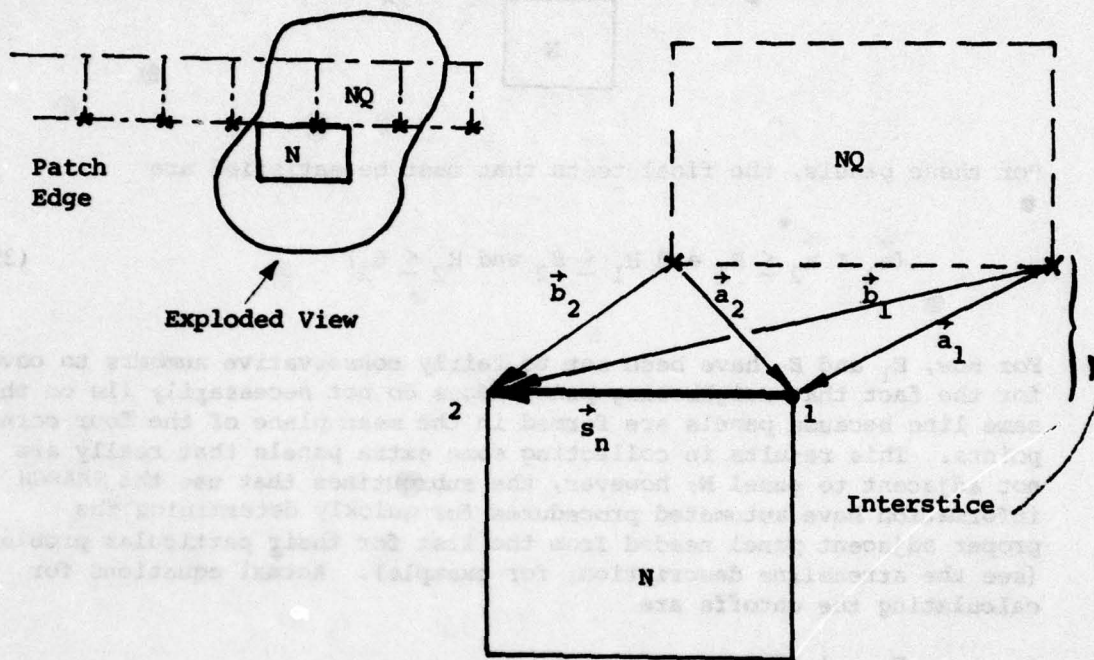
1. SEARCH identifies an array of panels along a patch edge adjacent to panel Q (multiple patches allowed).
2. The exiting panel is always used in setting up the partials associated with the next panel, NQ.
3. A new default intersection method insures an appropriate intersection.
4. Once an intersection point is found, this is used to locate the actual next panel, NQ, from the list of adjoining panels.
  - (a) Points in any interstices require that each possible next panel, NQ, is checked for streamline success.
  - (b) The new NQ must have participated in the calculation in getting across panel Q, or the process is repeated.
  - (c) The entering point is required to be on the edge of NQ.
5. A special technique is used for elements adjacent to a plane of symmetry.
6. Streamlines are stopped upon approaching a stagnation region.

Since each of the points representing a streamline is located at the boundary between two quadrilaterals, the values of the velocity and geodesic curvatures at each point can be computed separately for the two quadrilaterals. The average of the two values at a point is taken as the value at that point.

The streamline is first traced in the downstream direction, and then in the upstream direction. After the entire streamline has been obtained, the arc length along the streamline is computed so that it starts at zero at the upstream end. Points which are very close together are combined. Such points occur when the streamline cuts across a corner of a quadrilateral. If the distance between two points is less than one-eighth the distance between their neighbor in front and their neighbor in back, they are combined, and average values of their velocity, position, and curvatures are used for the new point.

# SEARCH ROUTINE

Since the body geometry is now represented by a number of patches, each containing its own independent, rectangular network of panels, it is necessary to be able to identify panels adjacent to each other across the patch edges; the user describes the patches and the particular sides of the patches that are joined together. Further, the panel identifiers along any side of a patch are calculated internally. In this way, searching for adjacent panels can be done efficiently. For example, if panels adjacent to panel N, say, on side 2 of patch x are to be found, then only panels on sides of the patches joined to side 2 of patch x need to be searched. The sketch below illustrates the method used to select adjacent panels.



To test whether NQ is a neighbor to N, the following quantities are first formed (see sketch for vector definitions):

$$D_i = (\vec{a}_i \cdot \vec{s}_n) (\vec{b}_i \cdot \vec{s}_n)$$

$$i = 1, 2$$

$$H_i = |\vec{a}_i \times \vec{s}_n|$$

$$i = 1, 2$$

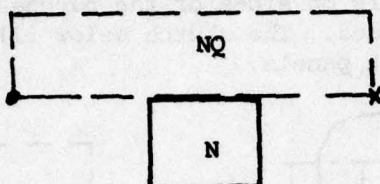
(37)

(No summation is implied here by double indices.) For NQ to be a neighbor to N,

$$(D_i \leq E_1 \text{ and } H_i \leq E_2)$$

$$i = 1 \text{ or } 2 \quad (38)$$

where  $E_1$  and  $E_2$  are small cutoff numbers which are discussed later. In the sketch above, this test would fail for  $i = 1$  but pass for  $i = 2$ , and NQ would be listed as a neighbor to N. If this test does fail for  $i = 1$  and  $i = 2$ , then a final test is made to recover NQ panels that might completely overlap panel N as indicated below:



For these panels, the final tests that must be satisfied are

$$(\vec{a}_1 \cdot \vec{a}_2 \leq E_1 \text{ and } H_1 \leq E_2 \text{ and } H_2 \leq E_2) \quad (39)$$

For now,  $E_1$  and  $E_2$  have been set to fairly conservative numbers to cover for the fact that neighboring panel edges do not necessarily lie on the same line because panels are formed in the mean plane of the four corner points. This results in collecting some extra panels that really are not adjacent to panel N; however, the subroutines that use the SEARCH information have automated procedures for quickly determining the proper adjacent panel needed from the list for their particular problem (see the streamline description, for example). Actual equations for calculating the cutoffs are

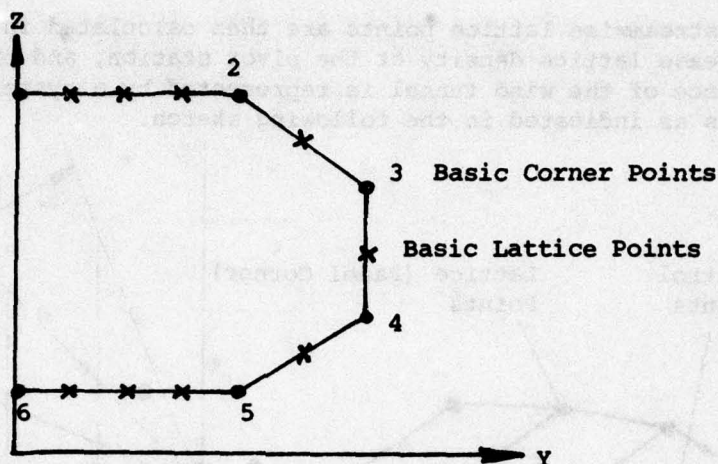
$$E_1 = 1.1(PD_N + PD_{NQ})$$

$$E_2 = S_N^2 + S_{NQ}^2$$

where PD is the projection distance used in generating the particular planar panel.

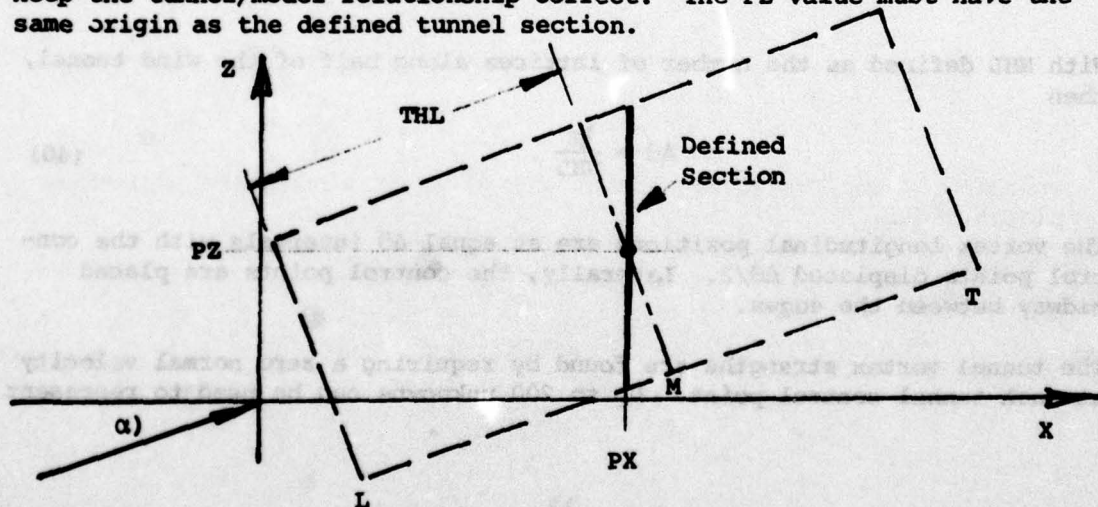
## WIND TUNNEL

The capability of modeling a body with wings (at zero sideslip) in a wind tunnel has been added to the program. In the tunnel option, the tunnel cross section is defined by a set of corner points. In between each corner point, a set of lattice points will be generated (see sketch below).



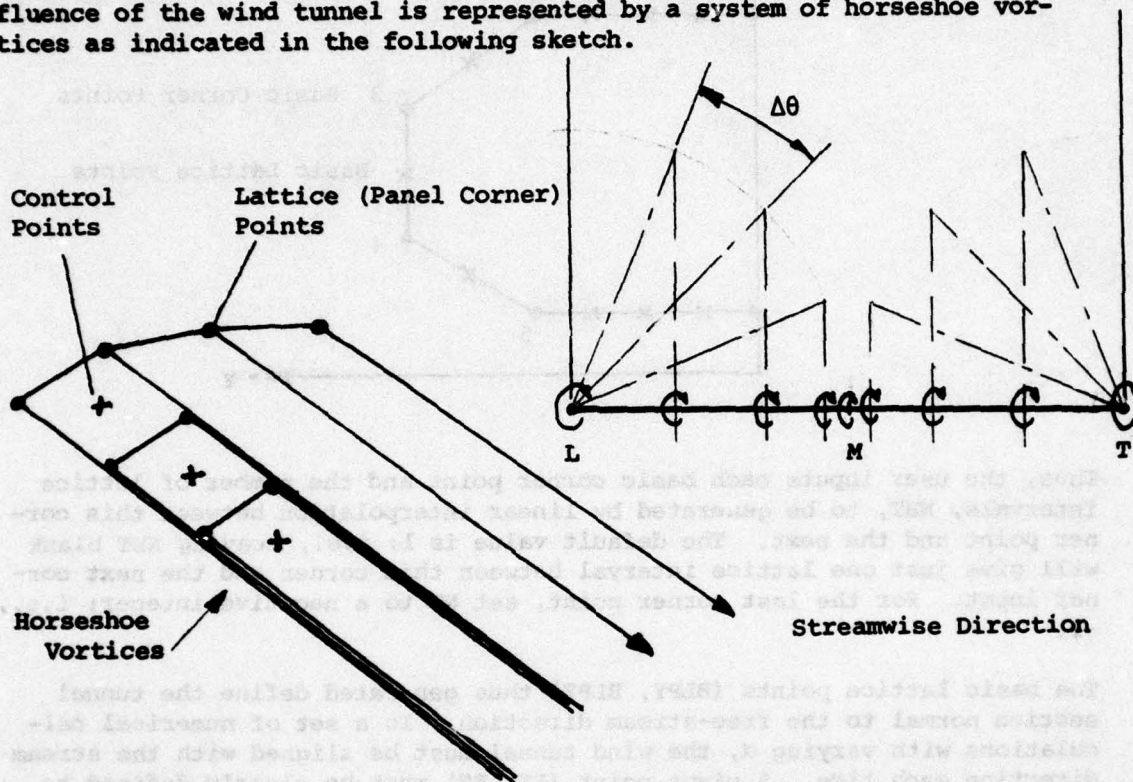
Thus, the user inputs each basic corner point and the number of lattice intervals, NBT, to be generated by linear interpolation between this corner point and the next. The default value is 1; i.e., leaving NBT blank will give just one lattice interval between this corner and the next corner input. For the last corner point, set NB to a negative integer; i.e., -1.

The basic lattice points (BLPY, BLPZ) thus generated define the tunnel section normal to the free-stream direction. In a set of numerical calculations with varying  $\alpha$ , the wind tunnel must be aligned with the stream direction each time. A pivot point (PX, PZ) must be clearly defined to keep the tunnel/model relationship correct. The PZ value must have the same origin as the defined tunnel section.



In rotating the defined section normal to the free stream, the y-ordinate remains unchanged. A new section at the pivot station, located at the mid station, M, is then generated (so as not to lose the basic one). Sections are also generated at the leading, L, and trailing, T, edges of the wind tunnel which are calculated from the tunnel half-length, THL, input by the user.

The streamwise lattice points are then calculated in a cosine spacing to increase lattice density at the pivot station, and the aerodynamic influence of the wind tunnel is represented by a system of horseshoe vortices as indicated in the following sketch.



With NHL defined as the number of lattices along half of the wind tunnel, then

$$\Delta\theta = \frac{\frac{1}{2}\pi}{\text{NHL}} . \quad (40)$$

The vortex longitudinal positions are at equal  $\Delta\theta$  intervals with the control points displaced  $\Delta\theta/2$ . Laterally, the control points are placed midway between the edges.

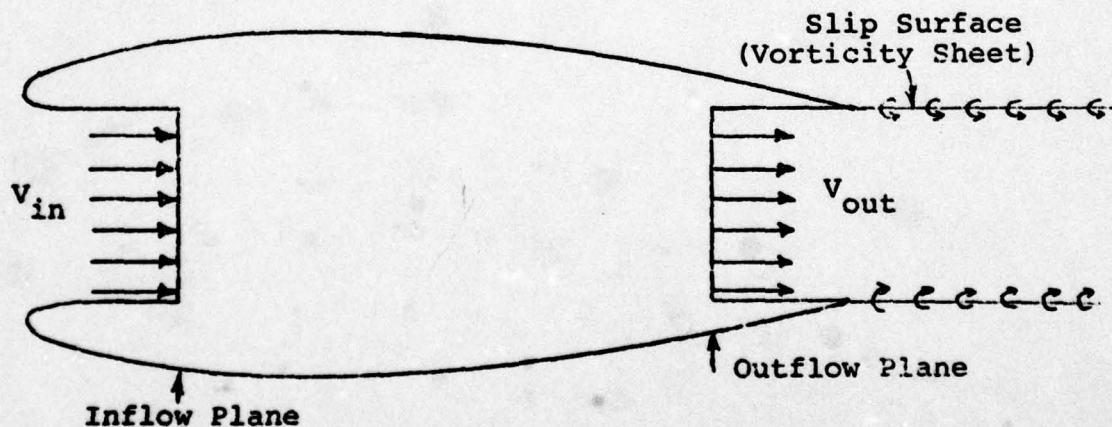
The tunnel vortex strengths are found by requiring a zero normal velocity at each tunnel control point. Up to 200 unknowns can be used to represent

the wind tunnel. The tunnel influences, along with all cross-coupling terms, have been assembled into the basic aerodynamic matrix as indicated below.

BODY	WING ON BODY	TUNNEL ON BODY
BODY ON WING	WING	TUNNEL ON WING
BODY ON TUNNEL	WING ON TUNNEL	TUNNEL

#### ENGINE INLET/EXHAUST REPRESENTATION

Because the engine inlet and exhaust of a helicopter configuration are generally an integral part of the fuselage flow field, it is important to model their influence in the analysis. A model that has been used successfully (Reference 6) is shown in the sketch below.



6. Geller, E.W., Dvorak, F.A., and Rizk, M., "Calculation of the Subsonic Flow about an Advanced Technology Transport and a Modified F-106B Aircraft", Flow Research Note No. 73, Prepared for NASA-Lewis Research Center, Contract NAS3-18341, April 1975.

The inlet and exhaust velocities (mass flow) are controlled using a prescribed normal velocity at panel control points in the inflow and outflow planes, respectively. The exhaust is enclosed within a vortex tube that represents the slip surface between the exhaust and outer flows. A good approximation to the vorticity value on the exhaust tube is  $\gamma = V_{out} - V_{\infty}$ , which assumes that the exit plane pressure is that of the free stream. The exhaust model is therefore basically the same as the separated flow model in this program, the main difference being the sign of the vorticity, since the former encloses a region of higher energy air and the latter encloses a region of lower energy air. The exhaust case, however, is somewhat easier than the drag case because the vorticity level is known approximately at the outset, being related to the engine mass flow.

A number of effluxes are allowed in the program. The user specifies the points around the edge of the jet outflow plane, the length of the efflux, and the vorticity strengths (i.e.,  $V_{OUT}$  or  $V_{JET}$ , approximately). The program generates a set of streamwise uniform vorticity panels on each efflux tube so defined. The influence of each efflux tube adds directly to the right side of the boundary condition equations, being an additional onset flow.

## APPLICATIONS

A preliminary version of the program DRAG has been used in two separate studies. In these studies, DRAG has been exercised in a manner much as it would be in an aircraft development program. A preliminary version of the code was used which had all of the features of the final version except that the constant source body singularities were retained. Execution of the program was identical to the version with the higher-order singularities, since these will be completely transparent to the user, requiring no special input. All the features of the program were exercised, cases being run with and without simulated wind tunnel effects, with normal flow through panels to simulate inlet and exhaust flows, with simulated efflux plumes, and with the panel addition and subtraction options being used. In addition, although not required for most helicopter configurations, the lifting surface portions of the program have been thoroughly evaluated. All of this work involved execution of the geometry, aerodynamic, streamline, and boundary layer calculation elements of the solution.

The program application was carried out under two separate studies. The first, funded under a subcontract to Hughes Helicopters, was a study of ways to reduce the drag of typical utility transport and armed attack helicopters through a program of progressive modification of the hub and pylon region. The second study involved the NAVY/ARPA/Lockheed X-Wing aircraft and was funded by the U.S. Naval Ship Research and Development Center (NSRDC). In both studies, the analysis was being used to analyze a baseline configuration and then to explore modifications to reduce the drag.

Panel models of the baseline configurations in the helicopter hub/pylon drag study are shown in Figures 3 and 4. The baseline utility transport helicopter model shown in Figure 3 was paneled by Sikorsky Aircraft under a separate Army-funded study, and as a consequence, is in the Sikorsky aerodynamic program format (Ref. 7). This presents no problem since the latest version of the DRAG program has the flexibility to read all or part of a model in the Sikorsky or the original WBAERO input format, or any mix of the two. The ability to read in the earlier XYZ program format has been retained (Ref. 8). The attack helicopter, shown in Figure 4, was set up from the beginning in the DRAG program input format.

- 
7. "Fuselage Geometry Definitions Program", Sikorsky Aircraft Report SER 50866, September 1974.
  8. Dawson, C.W., and Dean, J.S., "The XYZ Potential Flow Program", Naval Ship Research and Development Center (NSRDC) Report 3892, June 1972.

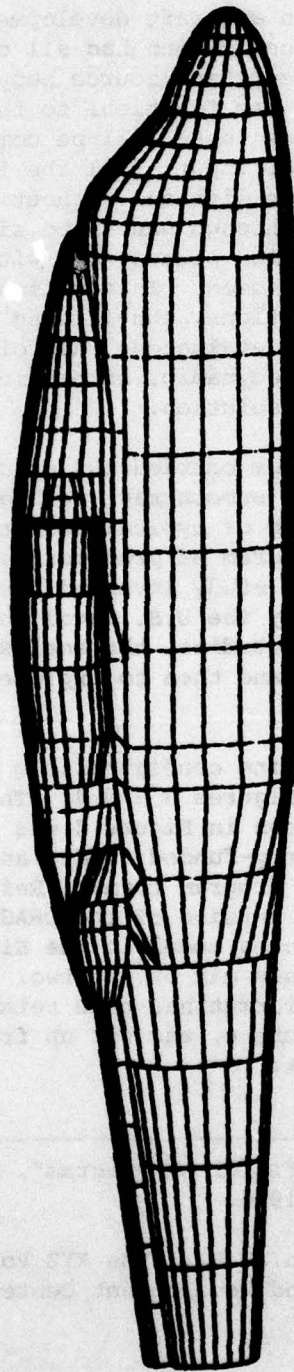


Figure 3. Panel Model of Typical Utility Transport Helicopter.

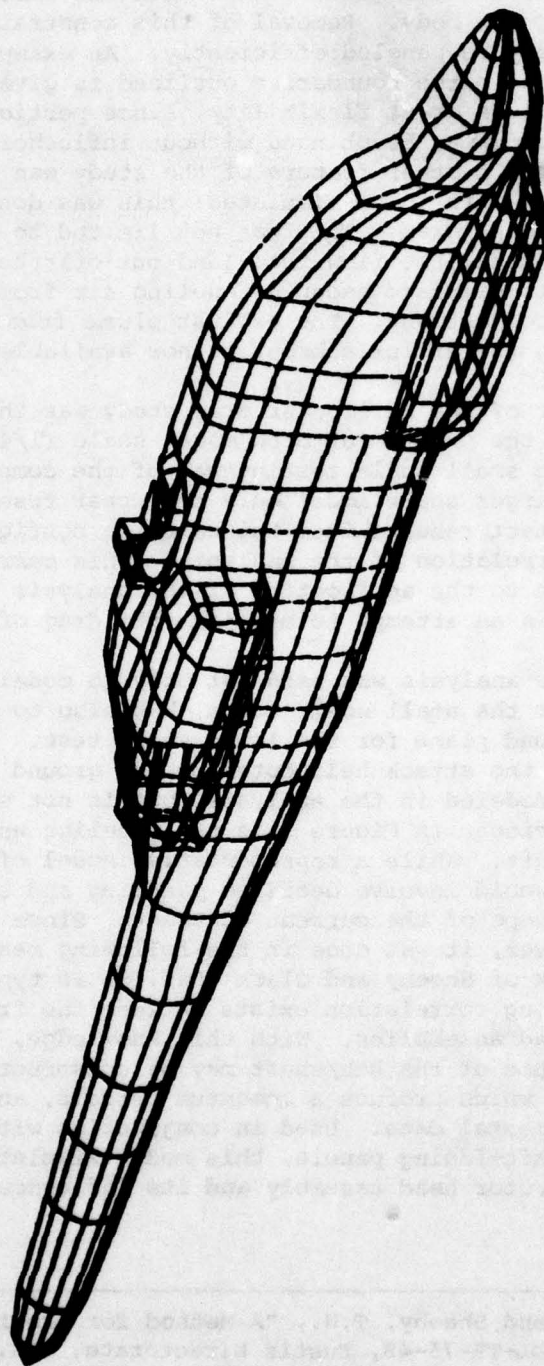


Figure 4. Panel Model of Typical Attack Helicopter.

Using the flexibility that the new code offers, both bodies have been set up using multi-patch paneling. This is an advance over the earlier version of the code where, in order to track streamlines, the paneling was constrained to a rectangular scheme with the same number of panels in each row along the body. Removal of this constraint means that complicated bodies may be paneled efficiently. An example of a multi-patch body with the patch boundaries outlined is given in Figure 1. Patching bodies gives great flexibility, since portions such as the pylon and upper body may be changed without influencing the rest of the configuration. Another feature of the study was that inlet and exhaust mass flows were to be simulated; this was done using the normal flow option in the program. This was not limited to engine flows, but was also used to model the flow into (and out of) the cavity around the rotor shaft and to simulate escaping cooling air from the attack helicopter avionics compartment. The exhaust plume from the power plants was modeled using the efflux subroutine now available in the program.

An important part of the helicopter drag study was the testing of models at each stage of the program at both model scale (1/4) and almost full (80%) scale. The small scale testing was of the complete aircraft, whereas in the larger scale model only the upper fuselage, pylon and hub were used. The test results from the baseline configurations will provide data for correlation of the analysis. This correlation is a necessary prelude to the application of the analysis in the later stages of the contract in an attempt to minimize the drag of both configurations.

Consequently, the analysis was used not only to model the complete baseline aircraft for the small scale tests, but also to model the partial model on the ground plane for the large scale test. Figure 5 shows the partial model of the attack helicopter on the ground plane. The wind tunnel was also modeled in the analysis, but is not shown here for clarity. Also evident in Figure 5 is the paneling used to model the rotor hub and shaft. While a representative model of the hub could be constructed, it would involve detailed paneling and separated flow modeling beyond the scope of the current contract. Since its presence must be modeled, however, it was done in the following manner. From earlier studies, the work of Sheehy and Clark (Ref. 9) is typical, it has been shown that a strong correlation exists between the frontal area and the drag of rotor head assemblies. With this knowledge, a crude panel model of the swept volume of the hub/shaft may be constructed and normal velocities prescribed which produce a momentum deficit, and hence a drag, to match the experimental data. Used in conjunction with the efflux model attached to the aft-facing panels, this model simulates very well the presence of the rotor head assembly and its influence on the surrounding surfaces.

---

9. Clark, D.R., and Sheehy, T.W., "A Method for Predicting Helicopter Hub Drag", USAAMRDL-TR-75-48, Eustis Directorate, U.S. Army Air Mobility Research and Development Laboratory, Ft. Eustis, Va., January 1976.

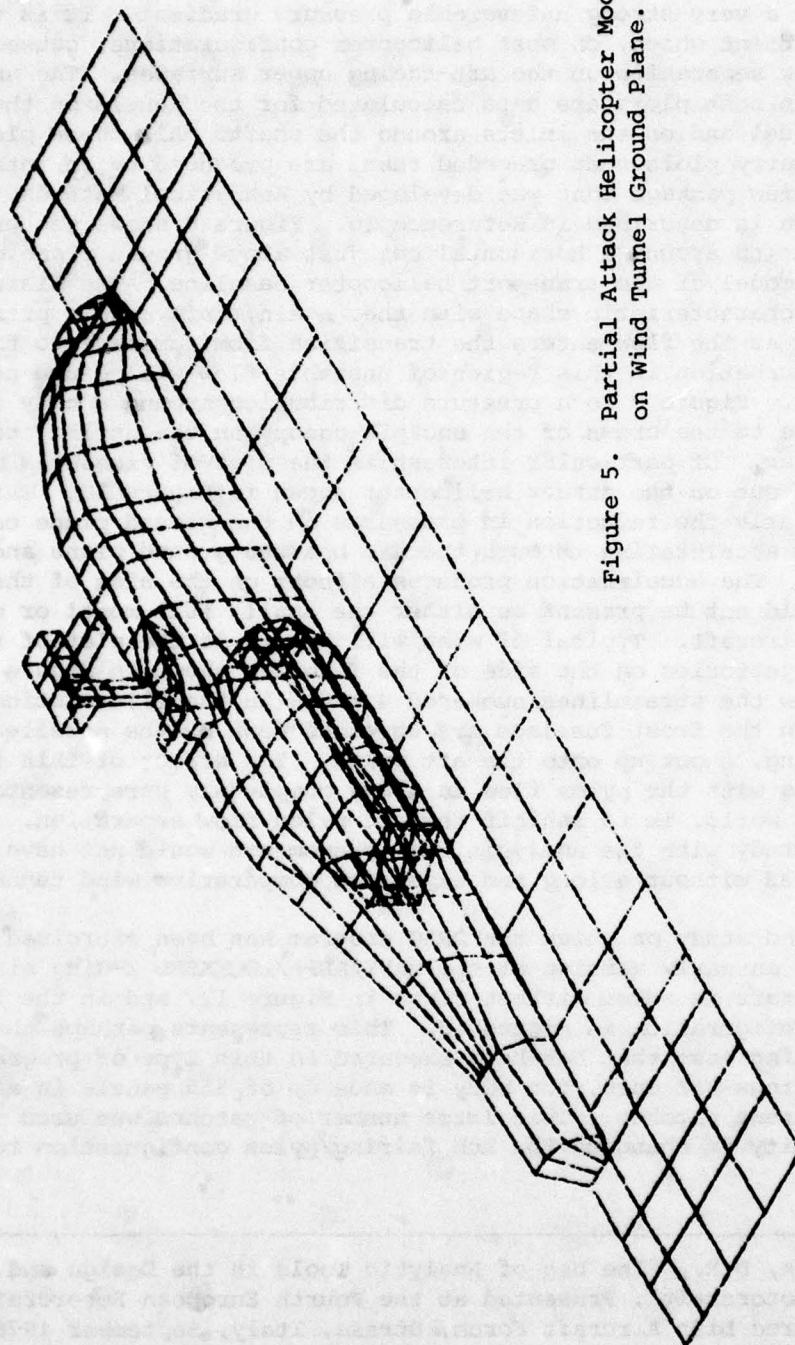


Figure 5. Partial Attack Helicopter Model  
on Wind Tunnel Ground Plane.

Some results from the rotor head drag study are given in Figures 6 through 10. In Figures 6 and 7, the centerline pressure distribution is given for the baseline utility and attack helicopters. Very clear in both plots in the region behind the rotor head and down the aft pylon is a very strong unfavorable pressure gradient. It is this pressure gradient which, on most helicopter configurations, causes the massive flow separation on the aft-facing upper surfaces. The unconnected points in both plots are data calculated for the panels on the hub and shaft model and on the inlets around the shaft. All these plots, and the geometry plots that preceded them, are produced by an interactive data review package that was developed by Analytical Methods, Inc., and which is described in Reference 10. Figure 8 shows the pressure distribution around a horizontal cut just above ground plane on the partial model of the transport helicopter baseline. The distribution has the characteristic shape with the, again, unfavorable pressure gradient as the flow enters the transition from fuselage to tail cone. Any perturbation in this region of unstable flow will cause separation and drag. Figure 9 is a pressure distribution around a body station cut close to the crown of the cockpit canopy on the utility transport helicopter. Of particular interest is the plot of pressures around a buttline cut on the attack helicopter shown in Figure 10. This shows very clearly the reduction in pressures on the ground plane caused by the flow accelerating through the gap between ground plane and engine nacelle. The acceleration produces effects on the side of the fuselage that would not be present on either the small, full model or on the actual aircraft. Typical of what will happen is the plot of the streamline trajectories on the side of the fuselage shown in Figure 11. This shows how the streamlines, numbered 4 and 5 in the illustration, originating on the front fuselage are squeezed down by the nacelle and then, recovering, shoot up onto the aft pylon. The effect of this flow, interacting with the pylon flow in a way completely unrepresentative of the real world, is to inhibit the aft pylon flow separation. Without the prestudy with the analysis this phenomenon would not have been discovered without a long and expensive comparative wind tunnel test.

The second study on which the DRAG program has been exercised is the study of an early version of the NAVY/ARPA/LOCKHEED X-Wing aircraft. The aircraft is shown without wings in Figure 12, and in the full, wings-fixed configuration in Figure 13. This represents perhaps the most challenging case that has been executed in this type of program to date. In the wings-off case, the body is made up of 565 panels in a total of 26 different patches. This large number of patches was used to provide flexibility in changing the hub fairing/pylon configuration to reduce

- 
10. Clark, D.R., "The Use of Analytic Tools in the Design and Development of Rotorcraft", Presented at the Fourth European Rotorcraft and Powered Lift Aircraft Forum, Stresa, Italy, September 1978.

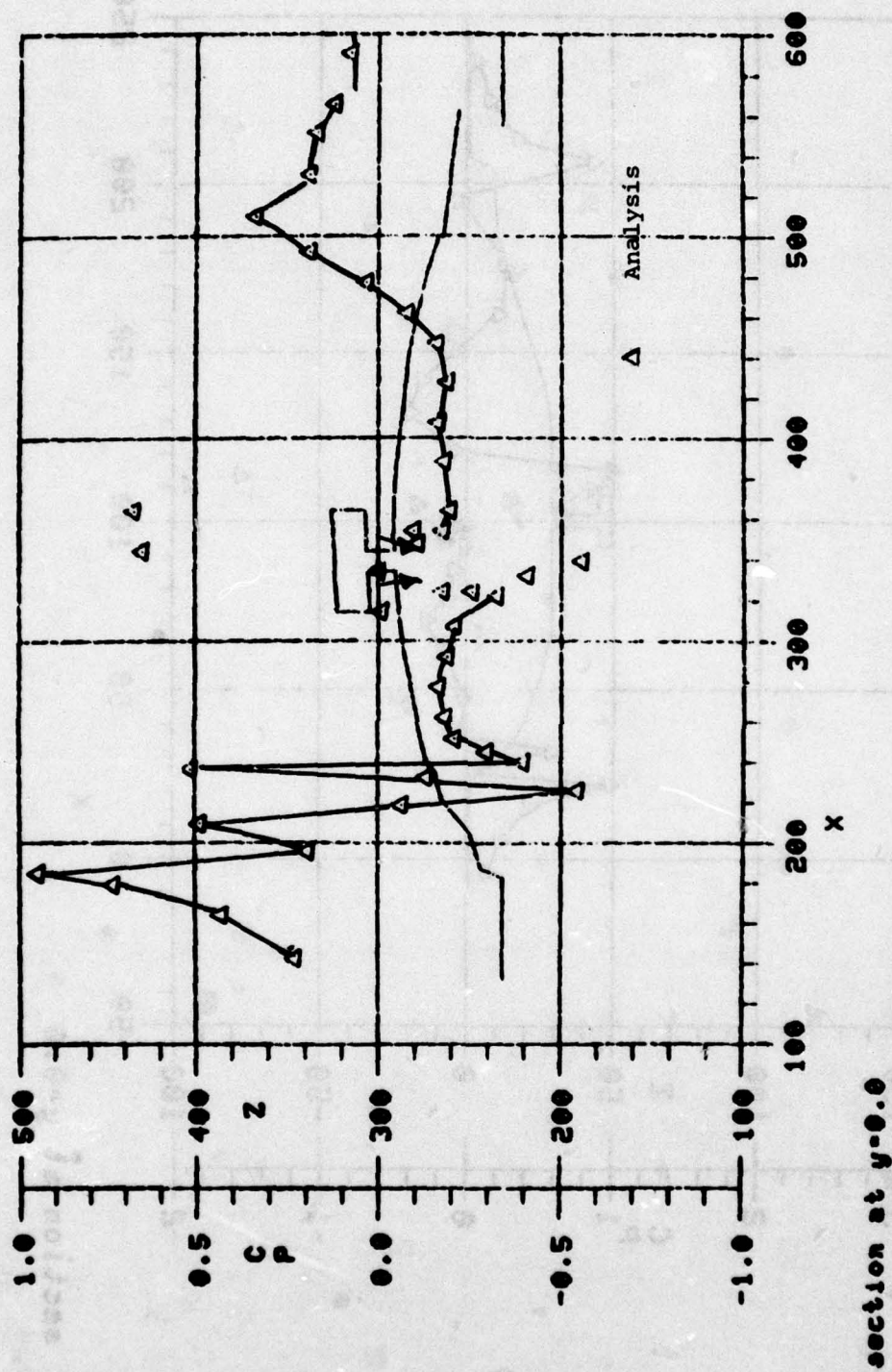


Figure 6. UH-60A Pressure Distribution Along Top Centerline.

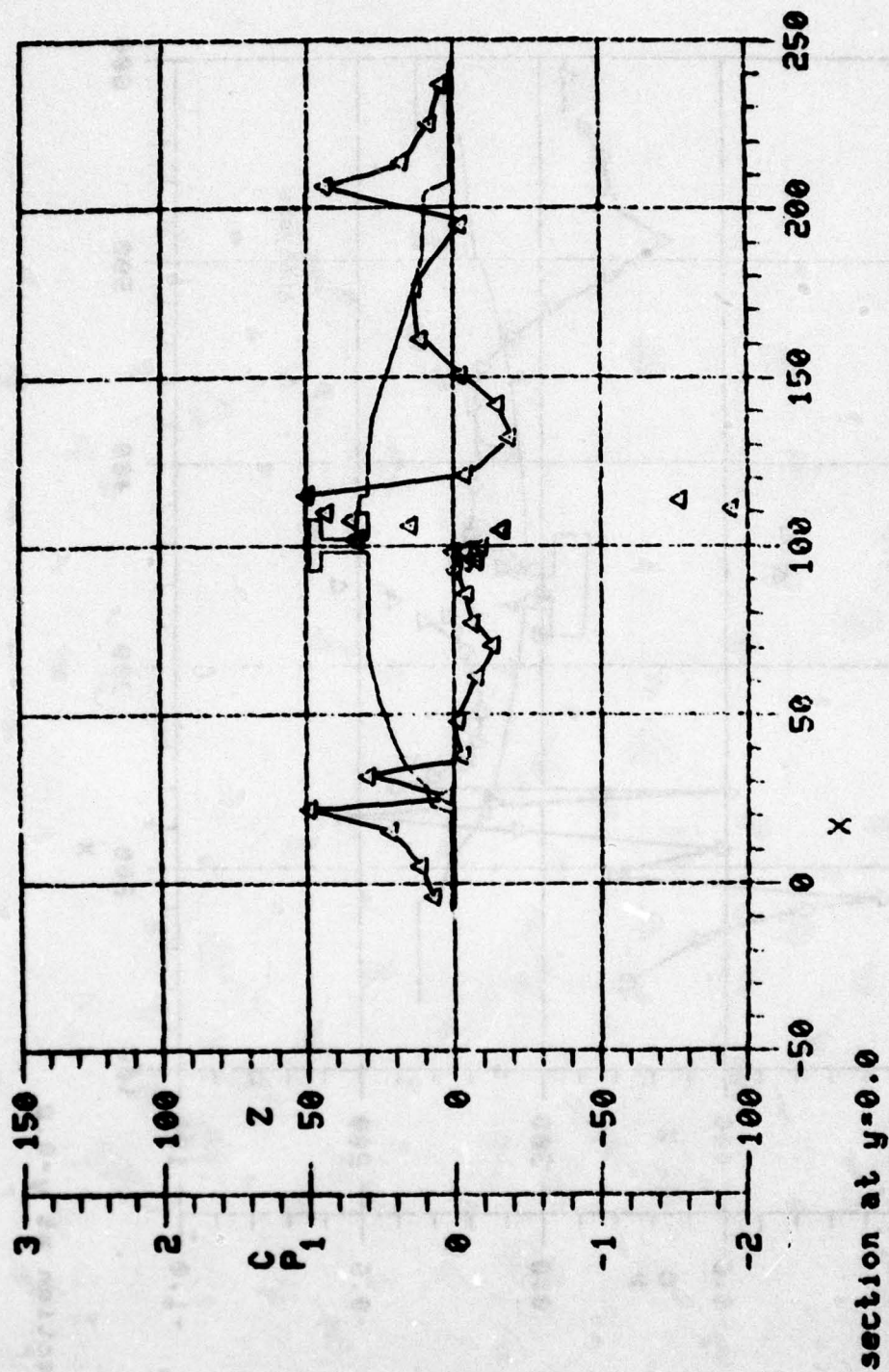


Figure 7. YAH-64 Pressure Distribution Along Top Centerline.

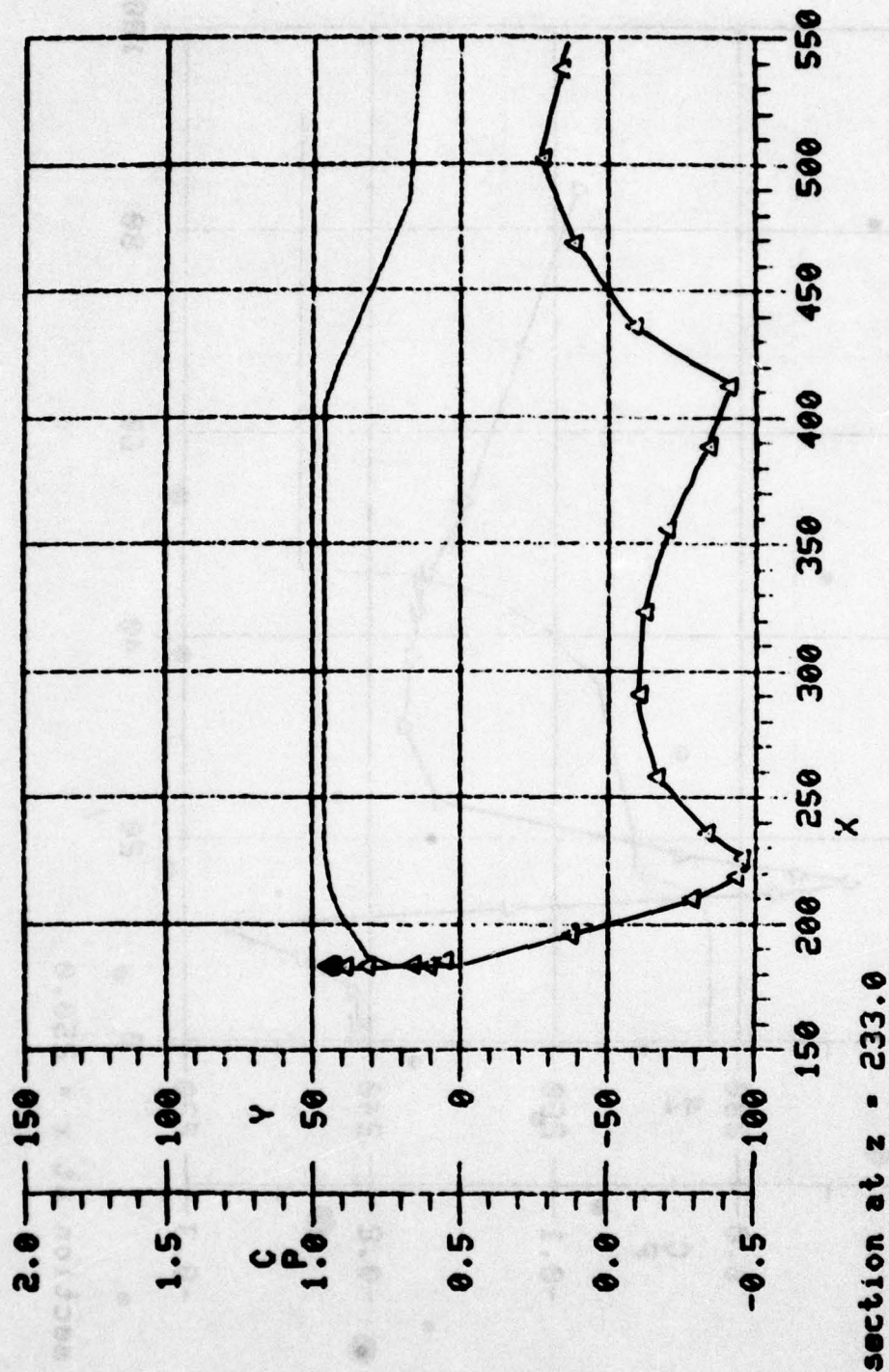


Figure 8. Pressure Distribution Above Ground Plane on Transport Helicopter Model.

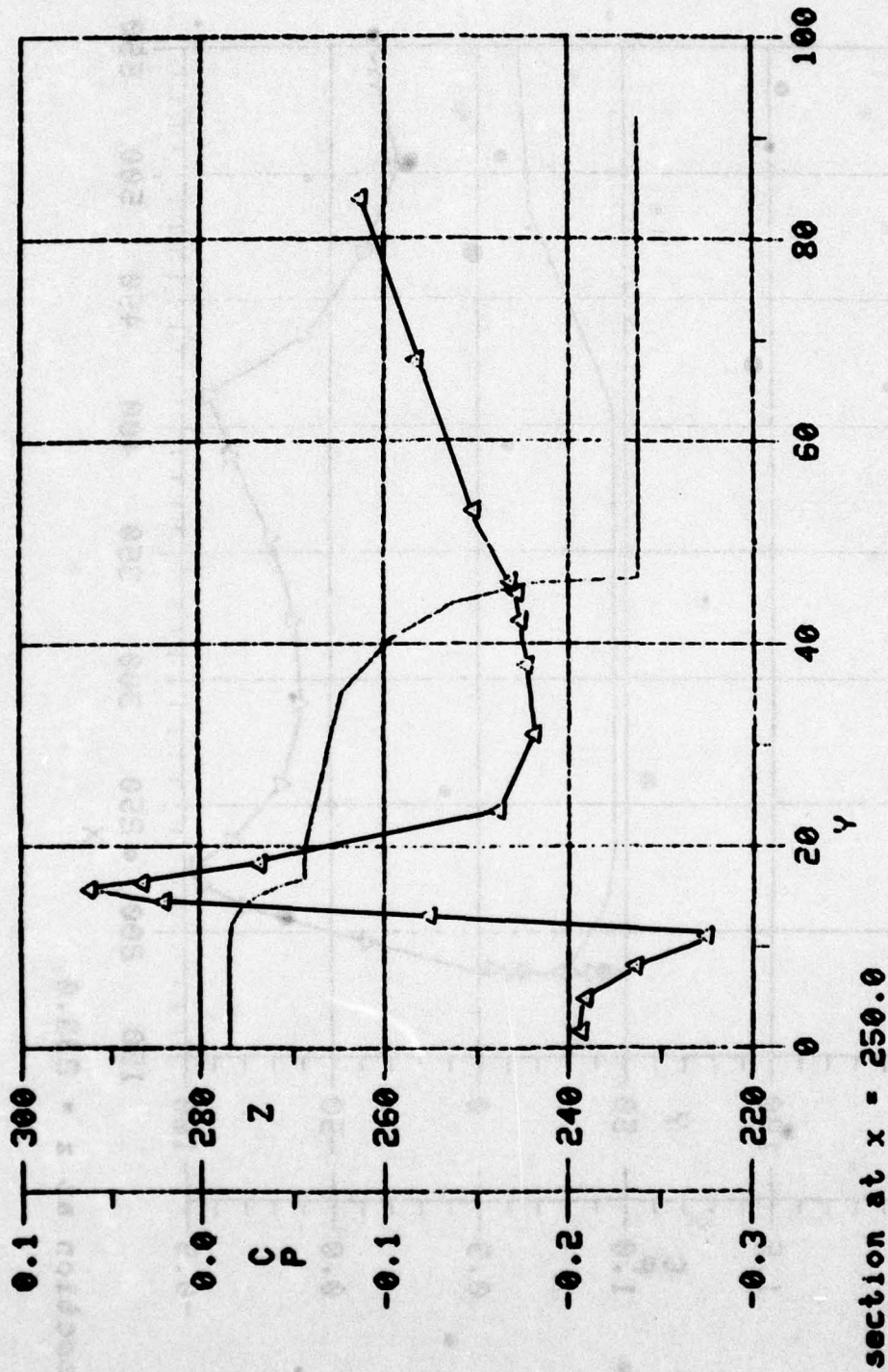


Figure 9. Pressure Distribution Around a Body Station Cut on Transport Helicopter Model.

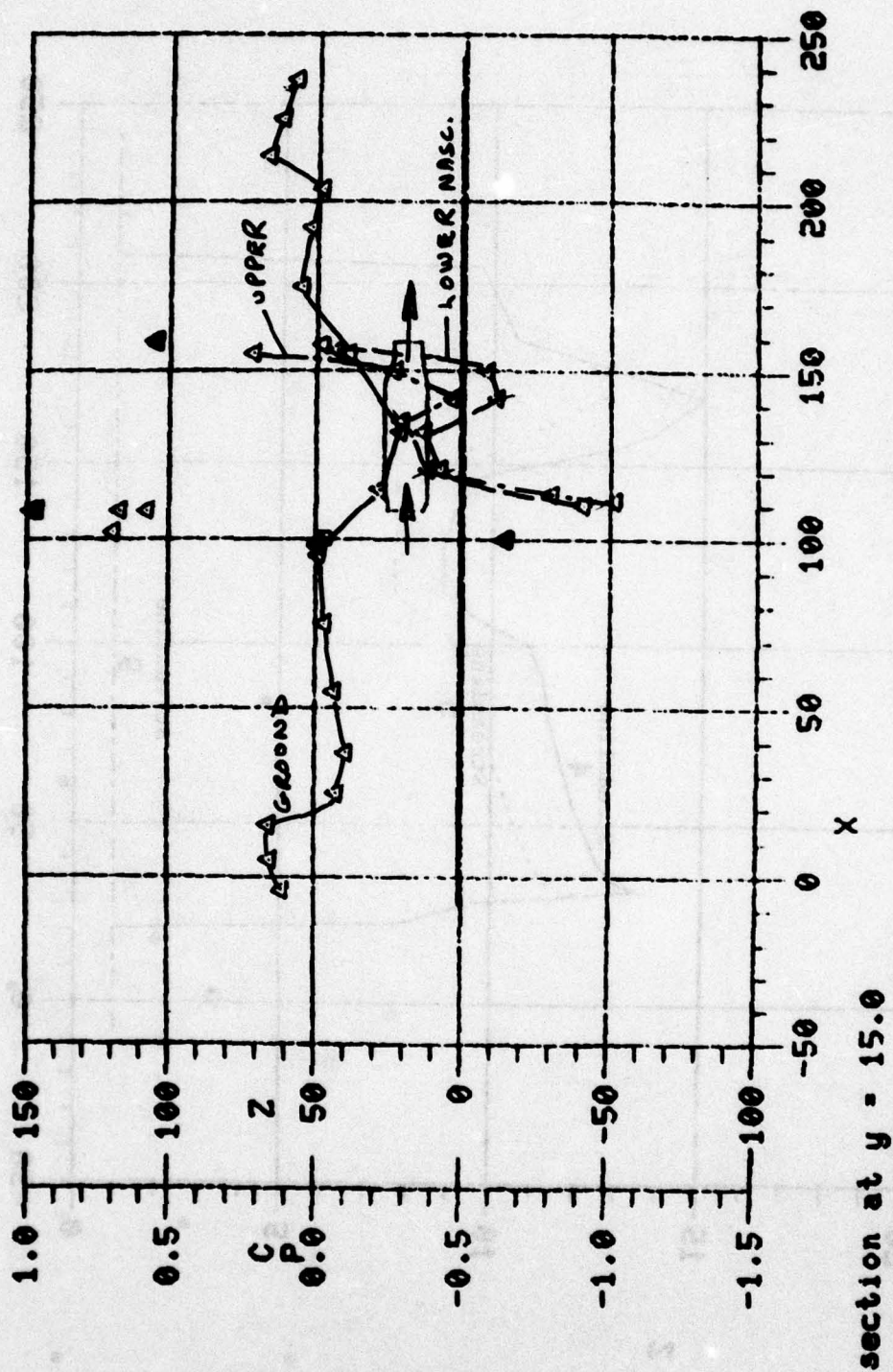


Figure 10. Pressure Distribution Around Buttline Cut on Attack Helicopter Model.

# STREAMLINE DATA

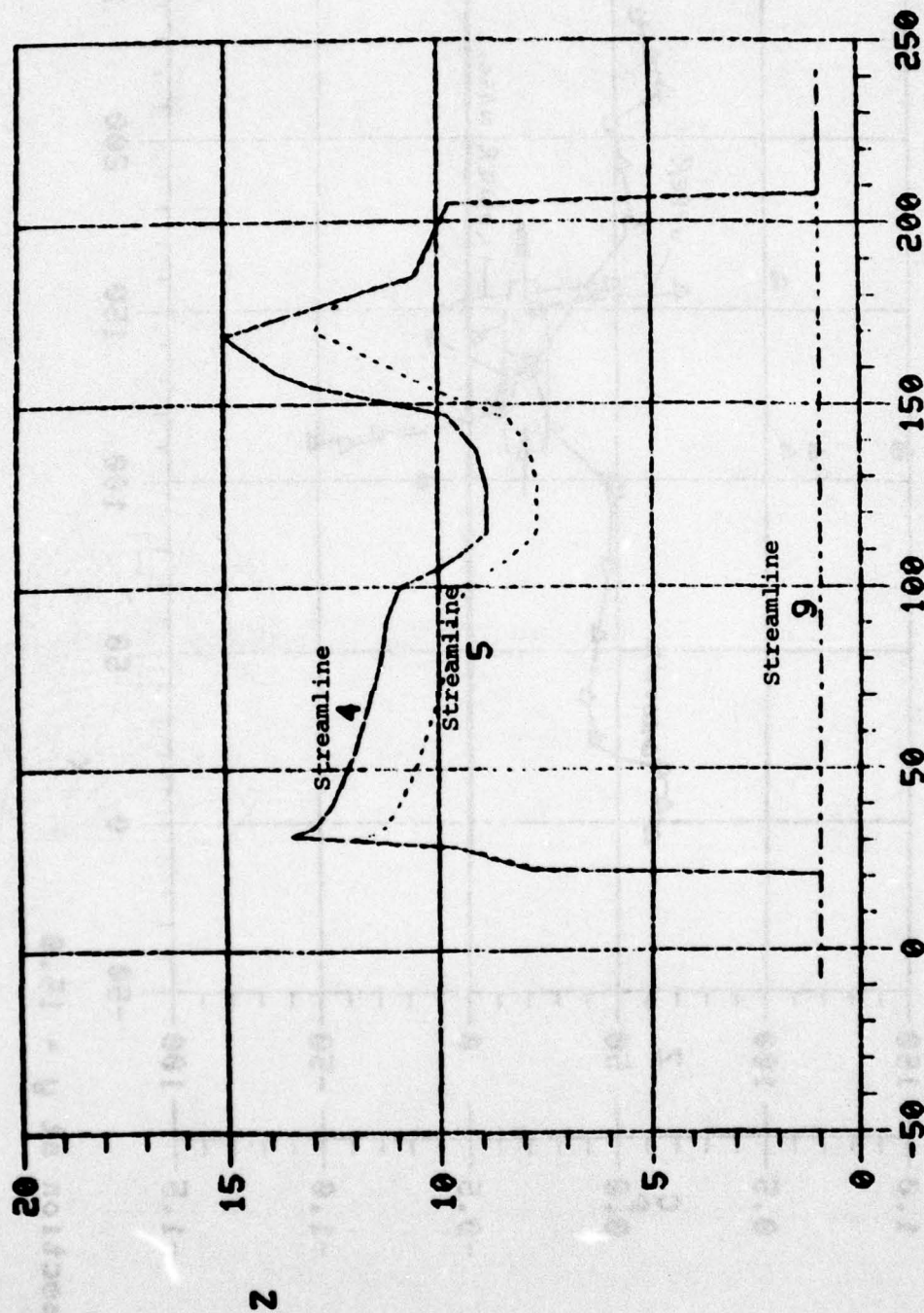


Figure 11. Streamline Trajectories on Side of Attack Helicopter Fuselage.

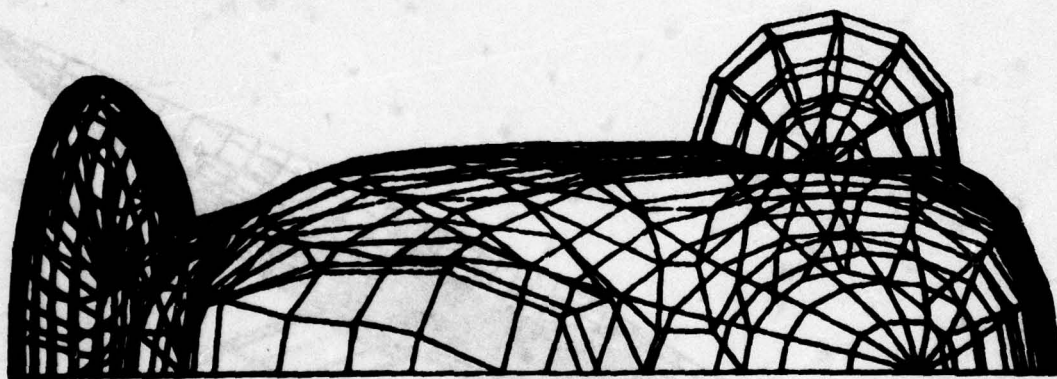


Figure 12. Navy/ARPA Lockheed X-Wing Front View Without Wings.

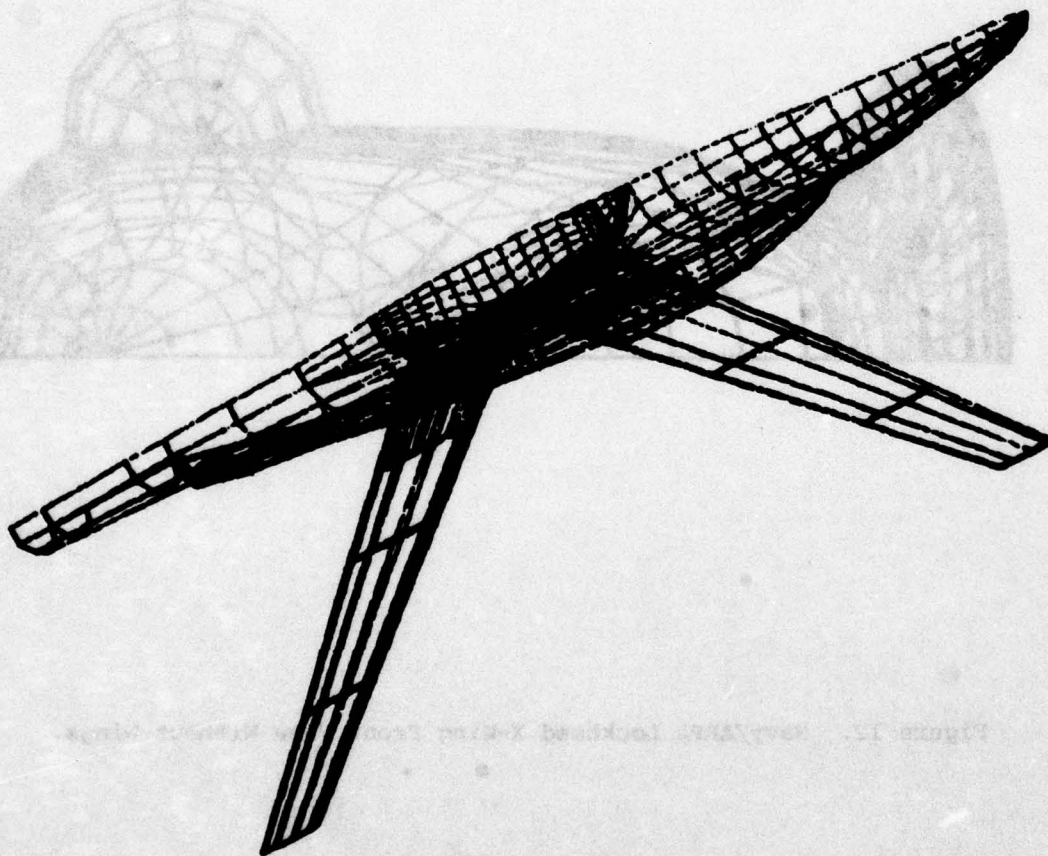
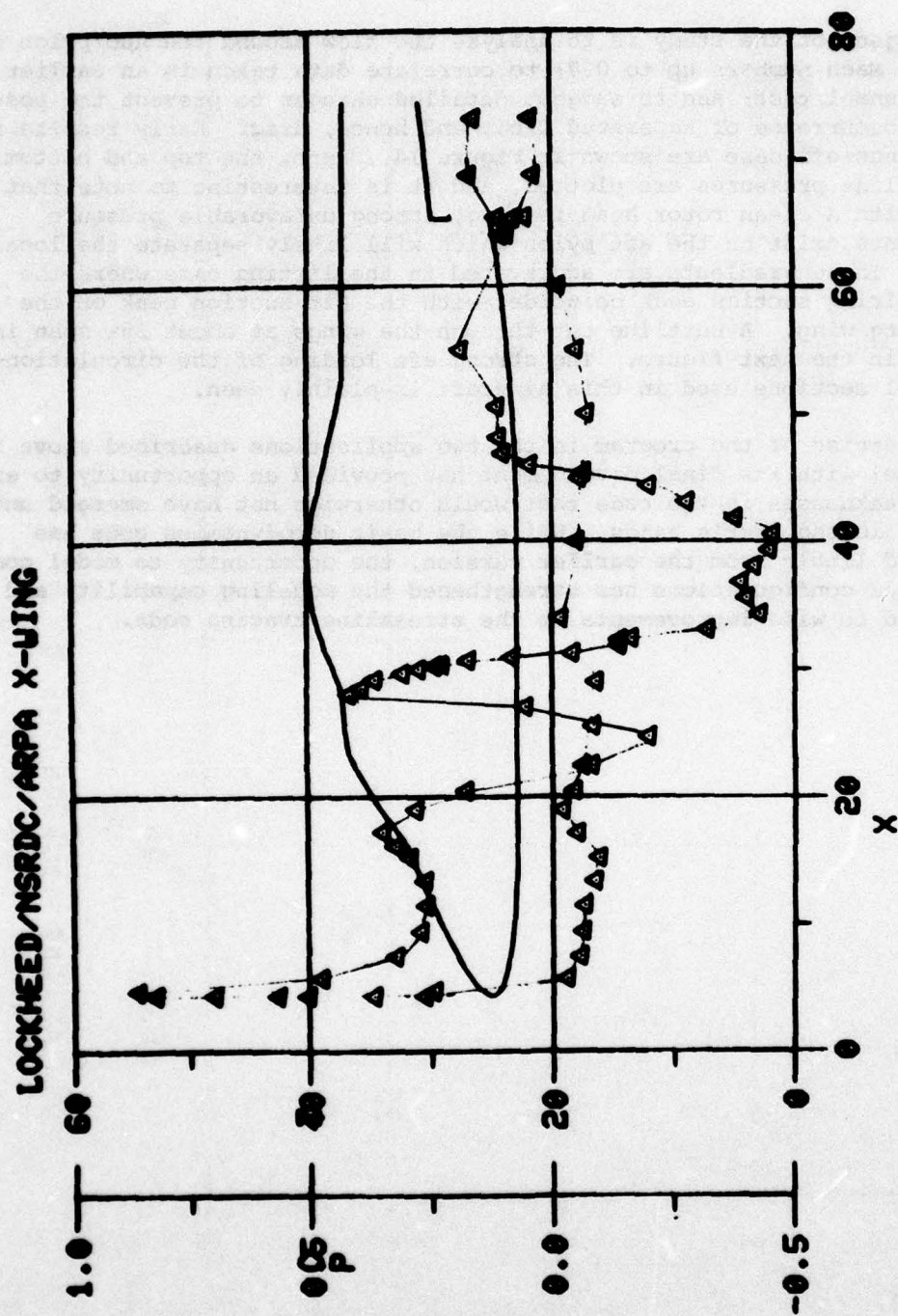


Figure 13. Navy/ARPA Lockheed X-Wing  
Full Configuration.

the drag. A total of 139 different input sections were used to build up the shape. With the fully lifting wings added, the number of panels is increased to 711.

The object of the study is to analyze the flow around the hub/pylon for flight Mach numbers up to 0.7; to correlate data taken in an earlier wind tunnel test; and to suggest detailed changes to prevent the possible occurrence of separated flow, and hence, drag. Early results for the wings-off case are shown in Figure 14. Here, the top and bottom centerline pressures are plotted, and it is interesting to note that even with a clean rotor head fairing, strong unfavorable pressure gradients exist on the aft pylon which will likely separate the local flow. These gradients are aggravated in the lifting case where the hub fairing suction peak coincides with the aft suction peak on the trailing wing. A buttline cut through the wings at about 25% span is shown in the next figure. The strong aft loading of the circulation-control sections used in this aircraft is plainly seen.

The exercise of the program in the two applications described above in parallel with its final development has provided an opportunity to expose weaknesses in the code that would otherwise not have emerged until it was in the user's hands. While the basic aerodynamics code has changed little from the earlier version, the opportunity to model complicated configurations has strengthened the modeling capability and has led to wide improvements in the streamline tracing code.



buttlne cut.Y-0.0 plot all data.

Figure 14. X-Wing Pressure Distributions Along Tip and Bottom Centerlines.

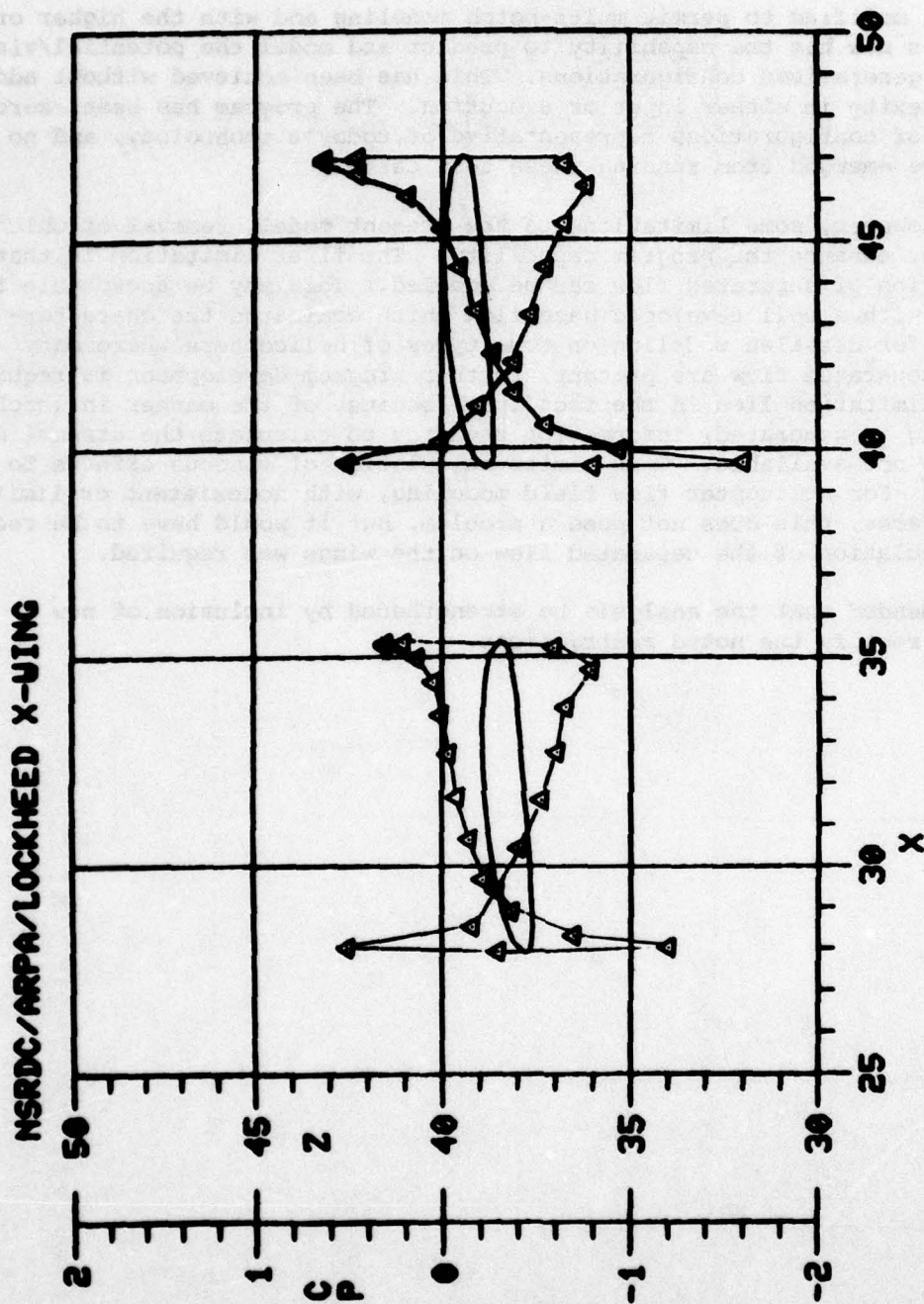


Figure 15. Pressure Distributions on Wings at 29% Span.

### CONCLUSIONS AND RECOMMENDATIONS

The analysis modified to permit multi-patch modeling and with the higher order singularities now has the capability to predict and model the potential/viscous flow around generalized configurations. This has been achieved without additional complexity in either input or execution. The program has been exercised on a number of configurations representative of today's technology, and no problems have emerged from running these test cases.

There are, however, some limitations to the present model, removal of which would further enhance the program capability. The first limitation is that only one region of separated flow can be modeled. This may be acceptable for some shapes with a well developed base flow which dominates the characteristics, but for detailed modeling on some types of helicopters where many regions of separated flow are present, further program development is required. The second limitation lies in the fact that, because of the manner in which wing paneling is generated, information required to calculate the streamline direction is not available. This limits calculation of viscous effects to the body panels. For helicopter flow field modeling, with nonexistent or limited lifting surfaces, this does not pose a problem, but it would have to be rectified if calculation of the separated flow on the wings was required.

It is recommended that the analysis be strengthened by inclusion of new elements to rectify the noted restrictions.

#### REFERENCES

1. Dvorak, F.A., Maskew, B., and Woodward, F.A., "Investigation of Three-Dimensional Flow Separation on Fuselage Configurations", USAAMRDL-TR-77-4, Eustis Directorate, U.S. Army Air Mobility Research and Development Laboratory, Fort Eustis, Va., March 1977, AD A039382.
2. Woodward, F.A., Dvorak, F.A., and Geller, E.W., "A Computer Program for Three-Dimensional Lifting Bodies in Subsonic Inviscid Flow", USAAMRDL-TR-74-18, Eustis Directorate, U.S. Army Air Mobility Research and Development Laboratory, Fort Eustis, Va., April 1974, AD 782202.
3. Maskew, B., and Dvorak, F.A., "The Prediction of  $C_{l_{max}}$  Using a Separated Flow Model", J. Am. Hel. Soc., April 1978.
4. Bristow, D.R., and Grose, G.G., "Modification of the Douglas Neumann Program to Improve the Efficiency of Predicting Component Interference and High Lift Characteristics", NASA CR-3020, January 1978.
5. Dawson, C.W., and Dean, J.S., "The Calculation of Streamline Data for Boundary Layer Input", NSRDC CMD-4-74, Naval Ship Research and Development Center, Bethesda, Md., January 1974.
6. Geller, E.W., Dvorak, F.A., and Rizk, M., "Calculation of the Subsonic Flow about an Advanced Technology Transport and a Modified F-106B Aircraft", Flow Research Note No. 73, Prepared for NASA-Lewis Research Center, Contract NAS3-18341, April 1975.
7. "Fuselage Geometry Definitions Program", Sikorsky Aircraft Report, SER 50866, September 1974.
8. Dawson, C.W., and Dean, J.S., "The XYZ Potential Flow Program", NSRDC Report 3892, Naval Ship Research and Development Center, Bethesda, Md., June 1972.
9. Clark, D.R., and Sheehy, T.W., "A Method for Predicting Helicopter Hub Drag", USAAMRDL-TR-75-48, Eustis Directorate, U.S. Army Air Mobility Research and Development Laboratory, Fort Eustis, Va., January 1976.
10. Clark, D.R., "The Use of Analytic Tools in the Design and Development of Rotorcraft", Presented at the Fourth European Rotorcraft and Powered Lift Aircraft Forum, Stresa, Italy, September 1978.

APPENDIX A

PROGRAM USER'S GUIDE

PROGRAM INPUT DESCRIPTION

<u>Card Set</u>	<u>Input</u>	<u>Format</u>
1.	Case Title	8A10
2.	RNB, TRIPUP, OPTION, TRMAX, XROUGH, REFC, UIN, XGEM	8F10.0
3.	UKU, DEN, XO, EPS, XNROUGH	7F10.0
4.	VRD(1) ... VRD(NROUGH)	7F10.0
5.	XPRINT, XSKIP, REFY, REFZ, CREF, PRINT, CASE	7F10.0
6.	NPANEL, NBX, MBX, NWX, MWX, NVX, MVX, ILX, NPTS, <u>NS</u>	10I5
7.	TEXT Card:- GEOMETRY INPUT	8A10
8.	CASE, PLOT, SIM, ISAVE, PRINT	5I10
9A.	SINGPA, NOPAN	2I10
9B.	X(I), Y(I), Z(I)	7F10.0
9C.	NPAN (1) ... NPAN(NOPAN)	7I10
10A.	NB	I10
10S1.	TYPE, TITLE(I)	18A4
10S2.	NOP, NIBI	2I10
10S3.	XOF, YOF, ZOF, XROT, ZROT	8F10.0
10S4.	AX(1), AY(1), AZ(1) ... ...AX(4), AY(4), AZ(4)	10X 6F10.0
10B.	XBE, YBE, ZBE, MB, OPT, FLAG	3F10.0, 3I10
10C.	B(J), A(J), D(J)	7F10.0
10D.	D(J), B(J), A(J)	3F12.0
11A.	NW, KOORD	2I10

<u>Card Set</u>	<u>Input</u>	<u>Format</u>
11B.	XBE, YBE, ZBE, CHRD, ALF, XAL, MW, OPT, FLAG, DEL	6F10, 4I5
11C.	DELTA, YO, ZO	7F10.0
11D.	B(J), A(J)	7F10.0
11E.	B(J), D(J), A(J), C(J)	5F12.0
12.	WAKE, POINT	7F10.0
13A.	XLP, YLP, ZLP	7F10.0
13B.	XLP, YLP, ZLP	7F10.0
14A.	NV	I10
14B.	XBE, YBE, ZBE, MV, OPT, FLAG, SIMPOT	3F10.0, 4I10
14C.	B(J), A(J), C(J), D(J)	7F10.0
14D1.	A, B, D	7F10.0
14D2.	A, B, D	7F10.0
14D3.	A, B, D	7F10.0
15.	TEXT Card:- AERODYNAMIC CALCULATIONS	8A10
16.	NIT, IEPS, ITYPE	3I10
17.	COMPT, SECT	2I10
18.	REFA, REFL, XOO, X25	7F10.0
19.	KUT, NBV, NV(1) ... NV(5)	7I10
20.	KOMPR, POINTS	2I10
21A.	NHL, PX, PZ, THL	I10, 3F10.0
21B.	YB, ZB, NBT	2F10.0, I5
22A.	NEFF	I10
22B.	EFL(M), EFGAM(M)	7F10.5
22C.	NPAN	10I5

<u>Card Set</u>	<u>Input</u>	<u>Format</u>
22D.	XE(I), YE(I), ZE(I)	7F10.5
23.	NMA	I10
24.	MA	7F10.0
25.	NAL	I10
26.	ALPHA, BETA	7F10.0
27.	IS	I10
28.	IA, IE	2I10
29.	IREI	I10
30.	II(1), II(2), ... ETC.	14I5
31.	DELY, REFL, XLE	7F10.0
32.	TEXT CARD:- STREAMLINE CALCULATIONS	8A10
33.	ENDFILE	I10
34.	NLIN, NSP(1), ... NSP(NLIN)	13I5
35A.	NJT	13I5
35B.	JOINT(I,J)	13I5
36.	6/7/8/9.	

## Description of Input Variables

Card 1:- General Identification. Card 1 contains any desired identifying information in Columns 1 - 80.

Card 2:- General Parameters.

<u>Column</u>	<u>Variable</u>	<u>Value</u>	<u>Description</u>
1-10	RNB	arbitrary	Reynolds number based on reference chord and free-stream velocity $U_{\infty}C/\nu \times (10^{-6})$  N.B. If the input geometry is in dimensional units, the Reynolds number will be input per unit; i.e., Re/inch
11-20	TRIPUP	"	Trip location (x/c)
		1.	No tripping desired
21-30	OPTION	0.	Boundary layer will trip where specified by TRIPUP
		1.	Program will test on boundary layer momentum thickness at trip location. If $R_{\theta} < 200$ , trip location will be repositioned to point where $R_{\theta} \geq 200$ . This deters the user from specifying an unrealistically early trip location.
31-40	TRMAX	arbitrary	Maximum number of iterations between inviscid and boundary layer modules
41-50	XROUGH	-1.	Standard boundary layer calculation for smooth surfaces
		0.	Boundary layer calculation with area suction (needs Cards 3 and 4)
		1.	Boundary layer calculation with surface roughness (needs Cards 3 and 4)
51-60	REFC	arbitrary	Reference chord in inches for determination of surface distance in INSPAN

<u>Column</u>	<u>Variable</u>	<u>Value</u>	<u>Description</u>
61-70	UIN	arbitrary	Free-stream velocity in feet per second for use in INSPAN
71-80	XGEM	0.	Standard case; program will execute for complete case
		1.	Program will assemble and print out geometry variables only and stop

N.B. REFC, UIN and XGEM currently not available.

Card 3:- Roughness Parameters.

<u>Column</u>	<u>Variable</u>	<u>Value</u>	<u>Description</u>
1-10	UKU	30.-70.	Value of roughness Reynolds number where effect of roughness is independent of viscosity (see Ref. 1)
11-20	DEN	2.-100.	Density of roughness element spacing (For sand grain roughness, use 3.175)
21-30	XO	.005-.02	Initial value of skin friction coefficient (.007 is usual starting value)
31-40	EPS	.0001	Error bound in skin friction calculation
41-50	XNROUGH	arbitrary	Number of input values of suction velocity, $v_w/U$ , or roughness heights, $k/c$

Card 4:- Roughness or Suction Distribution.

<u>Column</u>	<u>Variable</u>	<u>Value</u>	<u>Description</u>
1-10	VRD(1)	arbitrary (floating point)	Roughness height or area suction velocity ( $k/c$ or $V/U_\infty$ )
.	.	.	.
.	.	.	.
.	.	.	.
61-70	VRD(NROUGH)	"	"

Card 5:- General Parameters.

<u>Column</u>	<u>Variable</u>	<u>Value</u>	<u>Description</u>
1-10	XPRINT	0.	Suppresses printing of cross-flow integral thickness from IBL
		1.	Extra printing
11-20	XSKIP	1.	Print option in INTEGRAL; every integration step is printed
		10.	Every tenth step is printed
21-30	REFX	arbitrary	Reference (x/c) location for calculation of moment coefficient
31-40	REFZ	"	Reference (z/c) location for calculation of moment coefficient
41-50	CREF	1.	Redundant
51-60	PRINT	0.	"
61-70	CASE	1.	Number of angle-of-attack or Mach number variations for a given geometry. Currently limited to 1

Card 6:- Variable Dimension Options

<u>Column</u>	<u>Variable</u>	<u>Value</u>	<u>Description</u>
1-5	NPANEL	.LE.1500	Number of source panels and vortex lattices on one side of plane of symmetry
6-10	NBX	2-70	Number of body sections
11-15	MBX	3-60	Maximum number of input points for any body section
16-20	NWX	2-40	Number of wing sections
21-25	MWX	3-59	Maximum number of ordinates at any wing section
26-30	NVX	0-40	Number of streamwise vortices in body lattice
31-35	MVX	2-60	Number of bound vortices in body lattice

<u>Column</u>	<u>Variable</u>	<u>Value</u>	<u>Description</u>
36-40	ILX	2-35	Sum of wing and body lattices
41-45	NPTS	.LE.1500	Number of off-body points
46-50	NS	.LE.8	Number of streamlines

N.B. Great care should be taken in preparing this card since experience has shown that errors here are the most common cause of aborted runs. Too large a number selected causes machine capacity problems; too small gives inadequate array space and overwrites.

Geometry Input Cards:- If the configuration is symmetrical about the x,z plane, geometrical input is required for only one side of the configuration. The convention used herein is to present that half of the configuration lying on the positive y side of the x,z plane. If the configuration is not symmetric, complete geometrical input is required.

Card 7:- General Identification. Card 7 contains any desired identifying information in Columns 1 - 80.

Card 8:- Options Card.

<u>Column</u>	<u>Variable</u>	<u>Value</u>	<u>Description</u>
10	CASE	1	Isolated body only
		2	Isolated wing only
		3	Wing-body combinations
20	PLOT	0	No plot output (currently this is the only option available)
		1	Plot output requested
30	SIM	0	Configuration symmetric about x,z plane; panel geometry required on one side only (normal case)
		1	Configuration symmetric about x,z plane. Panel geometry input required on one side only; panel geometry output calculated for both sides. (Used when analyzing symmetric configuration in yaw.) Not currently available

<u>Column</u>	<u>Variable</u>	<u>Value</u>	<u>Description</u>
30	SIM	-1	Asymmetric configuration. Panel geometry input required for both sides
40	ISAVE	0	Geometry and influence coefficient matrices not saved
		1	Geometry and influence coefficient matrices saved in previous run to be used (TAPES 11 and 18 must be requested)
		-1	Geometry and influence coefficient matrices to be saved on TAPES 11 and 18
50	PRINT	0	Normal output
		1	Optional output 1. Includes panel geometry, coordinate transformation matrices, and panel forces and moments
		2	Optional output 2. Panel velocity components and influence coefficients. Requires <u>large line count limit</u>
		3	Optional output 3. The aerodynamic influence coefficient matrix, the right side of the matrix equation, and all solution iterations
		4	Optional output 4. This option prints out the successive solution iterations only

N.B. The normal output is always printed in addition to any optional output selected.

Card 9A:- Single Panel Control Card.

<u>Column</u>	<u>Variable</u>	<u>Value</u>	<u>Description</u>
1-10	SINGPA	0 1	No single panel input; omit Card Set 9B, continue reading input cards. Corner point coordinates of this panel follow on Card Set 9B
11-20	NOPAN	arbitrary integer	Number of panels to be deleted. If non-zero, panel indices follow on Card Set 9C

Card 9B:- Panel Corner Point Input.

<u>Column</u>	<u>Variable</u>	<u>Value</u>	<u>Description</u>
1-10	X(I)	arbitrary (floating point)	x-coordinate of corner I
11-20	Y(I)	"	y-coordinate of corner I
21-30	Z(I)	"	z-coordinate of corner I

Repeat Card 9B four times, once for each corner of the panel.

Card Set 9C:- Indices of Deleted Panels. NOPAN indices of deleted panels are read (7I10 format) if NOPAN > 0 on Card 9A. A maximum of 100 panels may be deleted. Wing and body vortex-lattice control panels may not be deleted.

**WARNING:** Great care should be taken when exercising this option when going to a streamline trace since dislocation of the row, column and panel counting can occur. Its use is not recommended until the user is completely familiar with program operation.

Card Set 10:- Body Panel Input. This card set allows the body panels to be calculated automatically from the section geometry data. Five options are available for inputting the section geometry. The XYZ program input referred to below conforms with the format of Reference 2. The Sikorsky input conforms to that outlined in Reference 9 for input to program Y 179C with minor additions outlined below (omit this Card Set if CASE = 2 on Card 8).

Card 10A:- Number of Body Sections.

<u>Column</u>	<u>Variable</u>	<u>Value</u>	<u>Description</u>
1-10	NB	arbitrary integer	Number of body sections ( $2 \leq NB \leq 140$ ) A negative number indicates Sikorsky input format

Card Set 10S1:- Alternate Sikorsky Input. This card set is entered by loading NB(10A) with a negative number. The value is not significant. Standard WBAERO/DRAG input may be resumed after reading Sikorsky input by reloading NB(10A) with the appropriate positive value. Panels should be grouped for input in regular arrays, as in a DRAG program patch, each patch of panels being separated by a Type/Title card (10S1), a panel count card (10S2) and a local origin and patch rotation card (10S3). To terminate a load in the Sikorsky input format, simply repeat the 10S Type Card Set appropriately.

Card 10S1:- Type/Title.

<u>Column</u>	<u>Variable</u>	<u>Value</u>	<u>Description</u>
1-4	TYPE	NL,S	Program expects nonlifting (body) panels, symmetric about centerline. (This is currently the only option available). Use on first input set only
		BLANK	Normal input sets
		END	Terminates Sikorsky input
5-80	TITLE	alphabetic	Any title

Card Set 10S2:- Panel/Row Counting.

<u>Column</u>	<u>Variable</u>	<u>Value</u>	<u>Description</u>
1-10	NOP	arbitrary integer	Number of panels in patch
11-20	MBI	arbitrary integer	Number of panels in each column of the patch

Card 10S3:- Offsets and Rotation.

<u>Column</u>	<u>Variable</u>	<u>Value</u>	<u>Description</u>
1-10	XOF	arbitrary (floating point)	x-coordinate of patch local origin
11-20	YOF	"	y-coordinate of patch local origin
21-30	ZOF	"	z-coordinate of patch local origin

<u>Column</u>	<u>Variable</u>	<u>Value</u>	<u>Description</u>
31-40	XROT	arbitrary (floating point)	Angle in degrees which input points should be rotated about x-axis
41-50	ZROT	"	Angle in degrees which input points should be rotated about z-axis

Card Set 10S4:- Panel Corner Points.

Card 10S4,1.

<u>Column</u>	<u>Variable</u>	<u>Value</u>	<u>Description</u>
1-10	BLANK		May be used for panel identification
11-20	AX(1)	arbitrary (floating point)	Ordinates of first corner point on first panel
21-30	AY(1)	"	"
31-40	AZ(1)	"	"
41-50	AX(2)	"	Ordinates of second corner point on first panel
51-60	AY(2)	"	"
61-70	AZ(2)	"	"

Card 10S4,2.

<u>Column</u>	<u>Variable</u>	<u>Value</u>	<u>Description</u>
1-10	BLANK		
11-20	AX(3)	arbitrary (floating point)	Ordinates of third corner point on first panel
21-30	AY(3)	"	"
31-40	AZ(3)	"	"
41-50	AX(4)	"	Ordinates of fourth corner point on first panel

<u>Column</u>	<u>Variable</u>	<u>Value</u>	<u>Description</u>
51-60	AY(4)	arbitrary (floating point)	Ordinates of fourth corner point on first panel
61-70	AZ(4)	"	"

Repeat Card Set 10S4 NOP times to complete the input for each patch.

Repeat Card Set 10S for each patch to be loaded.

To terminate Sikorsky input, load Card 10S1 with TYPE = END.

Card 10B:- Body Section Geometry.

<u>Column</u>	<u>Variable</u>	<u>Value</u>	<u>Description</u>
1-10	XBE	arbitrary (floating point)	x-coordinate of origin of body section coordinate system, except blank when XYZ program input format is used
11-20	YBE	"	Similarly the y-coordinate
21-30	ZBE	"	Similarly the z-coordinate
31-40	MB	arbitrary integer	Number of input points on section ( $3 \leq MB \leq 60$ )  If $MB < 0$ , XYZ program input format re- quested
50	OPT	0	Body section geometry input by y-z co- ordinates on Card Set 10C and 10D
		1	Body section geometry same as preceding body section - Card Set 10C or 10D omitted. Note: YBE and ZBE are addi- tive to preceding values
		2	Body section geometry input in polar coordinates, $r$ , $\theta$ , on Card Set 10C
		3	Body of revolution, section geometry input as section radius and theta incre- ment on Card Set 10C

<u>Column</u>	<u>Variable</u>	<u>Value</u>	<u>Description</u>
60	FLAG	0	Normal body section
		1	Terminal body section (end of current body panel network)
		2	End of rectangular grid

Card Set 10C:- Body Section Coordinates (Normal Input).

<u>Column</u>	<u>Variable</u>	<u>Value</u>	<u>Description</u>
1-10	B(J)	arbitrary (floating point)	y-coordinate of point J if OPT = 0; or angular coordinate (in degrees) of J if OPT = 2; or increment angle, $\Delta\theta$ , in degrees if OPT = 3
11-20	A(J)	"	z-coordinate of point J if OPT = 0; or r-coordinate of point J if OPT = 2; or body section radius if OPT = 3
21-30	D(J)	"	$\Delta x$ shift of point J if OPT = 0 or 2

Card Set 10C contains MB cards if OPT = 0 or 2; contains only 1 card if OPT = 3; and is omitted if OPT = 1 or MB < 0 on Card 10B.

Card Set 10D:- Alternate ZYZ Input.

<u>Column</u>	<u>Variable</u>	<u>Value</u>	<u>Description</u>
1-12	D(J)	arbitrary (floating point)	x-coordinate of point J
13-24	B(J)	"	y-coordinate of Point J
25-36	A(J)	"	z-coordinate of point J

This card set is omitted unless MB < 0 in card 10B.

Note: Repeat Card 10B and Card Sets 10C or 10D NB times to complete Card Set 10.

Card 11A:- Number of Wing Sections.

<u>Column</u>	<u>Variable</u>	<u>Value</u>	<u>Description</u>
1-10	NW	arbitrary integer	Number of wing sections ( $2 \leq NW \leq 40$ )
20	KOORD	1	Wing section ordinates input in percent of local chord
		2	Wing section ordinates input are not normalized

Card 11B:- Wing Section Geometry.

<u>Column</u>	<u>Variable</u>	<u>Value</u>	<u>Description</u>
1-10	XBE	arbitrary (floating point)	x-coordinate of origin of wing section coordinate system
11-20	YBE	"	Similarly the y-coordinate
21-30	ZBE	"	Similarly the z-coordinate
31-40	CHRD	"	Chord length section
41-50	ALF	arbitrary (floating point)	Section twist angle (degrees) or flap rotation angle. (Degrees positive for positive flap deflection)
51-60	XAL	"	Center of twist or rotation in percent chord
61-65	MW	arbitrary integer	Number of coordinates in section ( $5 \leq MW \leq 59$ )
70	OPT	0	Wing section ordinates to be used from card set 11D
		1	Wing section ordinates same as preceding section - card set 11D omitted
75	FLAG	0	Normal case - surface vorticity calculated automatically
		1	Terminal wing section (end of current wing panel network)

<u>Column</u>	<u>Variable</u>	<u>Value</u>	<u>Description</u>
75	FLAG	2	No vortex-lattice panels calculated for this section
		3	The coordinates of the last bound vortex in the vortex lattice are read in on Card 13 for this section
80	DEL	0	No wing dihedral
		1	Dihedral input on Card Set 11C

Card Set 11C:- Wing Dihedral Input.

<u>Column</u>	<u>Variable</u>	<u>Value</u>	<u>Description</u>
1-10	DELTA	arbitrary (floating point)	Dihedral angle (degrees)
11-20	YO	"	y- and z-ordinates of axis of rotation of wing panel
21-30	ZO	"	

N.B. Omit Card Set 11C if DEL = 0 in Card 11B.

Card Set 11D:- Wing Section Coordinates.

<u>Column</u>	<u>Variable</u>	<u>Value</u>	<u>Description</u>
1-10	B(J)	arbitrary (floating point)	x-coordinates of point J
11-20	A(J)	"	z-coordinate of point J

N.B. Card Set 11D contains MW cards of OPT = 0, and is omitted if OPT = 1. Repeat Card 11B and Card Sets 11C and 11D NW times to complete Card Set 11.

Card Set 12:- Vortex-Lattice Control Point Location.

<u>Column</u>	<u>Variable</u>	<u>Value</u>	<u>Description</u>
1-10	WAKE	arbitrary (floating point)	Extension of vortex lattice into wake in percent chord (usually 100.)
11-20	POINT	"	Location of vortex-lattice control point in percent chord behind trailing edge (usually .1)

N.B. These values are not used if FLAG = 3 on Card 11B.

Card Set 13:- Relocation of Vortex-Lattice Terminal Points. This Card Set is omitted unless FLAG = 3 on Card 11B. For each wing section having FLAG = 3, two additional cards are required to specify the terminal points of the streamwise vortices.

Card Set 13A:- Inboard Terminal Points.

<u>Column</u>	<u>Variable</u>	<u>Value</u>	<u>Description</u>
1-10	XLP	arbitrary (floating point)	x-coordinate of inboard edge of lattice terminal point
11-20	YLP	"	y-coordinate of inboard edge of lattice terminal point
21-30	ZLP	"	z-coordinate of inboard edge of lattice terminal point

Card Set 13B:- Outboard Terminal Points. Same as Card 13A for outboard edge of lattice terminal point.

Card Set 14:- Body Vortex-Lattice Input. This Card Set allows additional vortex lattices to be located inside the body of wing-body combinations, and is omitted if CASE < 3 on Card 8.

Card Set 14A:- Number of Streamwise Vortices in Body Vortex-Lattice Network.

<u>Column</u>	<u>Variable</u>	<u>Value</u>	<u>Description</u>
1-10	NV	arbitrary integer	Number of streamwise vortices in body vortex-lattice network ( $NV \leq 40$ )

Note: The sum of all wing and body vortex lattices may not exceed 35.

Card Set 14B:- Vortex-Lattice Geometry.

<u>Column</u>	<u>Variable</u>	<u>Value</u>	<u>Description</u>
1-10	XBE	arbitrary (floating point)	x-coordinate of origin of streamwise vortex
11-20	YBE	"	y-coordinate of origin of streamwise vortex
21-30	ZBE	"	z-coordinate of origin of streamwise vortex
31-40	MV	arbitrary integer	Number of bound vortices in lattice $2 \leq MV \leq 60$
41-50	OPT	0	Vortex-lattice points to be read from Card Set 14C
		1	Vortex-lattice points same as preceding. Omit Card Set 14C
		2	Optional vortex-lattice control panel coordinates read on Card 14D3
51-60	FLAG	0	Normal case - vortex-lattice panels calculated
		1	Terminal vortex of current body vortex-lattice network
		2	Corner points of control point panel to be read on Cards 14D2 and 14D3 (used when arbitrary control point is desired)

<u>Column</u>	<u>Variable</u>	<u>Value</u>	<u>Description</u>
61-70	SIMPOT	0	Symmetry option specified on Card 8 enforced for this vortex
		1	Symmetry option ignored for this vortex lattice (used for inserting vortex-lattice networks in vertical tails located in x,z plane)

**Card Set 14C:- Vortex-Lattice Coordinates.**

<u>Column</u>	<u>Variable</u>	<u>Value</u>	<u>Description</u>
1-10	B(J)	arbitrary (floating point)	x-coordinate of point J
11-20	A(J)	"	z-coordinate of point J
21-30	C(J)	"	Vortex-lattice strength at point J
31-40	D(J)	"	$\Delta y$ shift of point J

Card Set 14C contains MV cards if OPT = 0, and is omitted if OPT = 1 on Card 14B.

**Control Set 14D:- Vortex-Lattice Terminal Point and Control Point Coordinates.** Two or three additional cards are required to specify the terminal point of the streamwise vortex, and the corner points of the lattice control point panel.

**Card 14D1.**

<u>Column</u>	<u>Variable</u>	<u>Value</u>	<u>Description</u>
1-10	B	arbitrary (floating point)	x-coordinate of terminal point of streamwise vortex
11-20	A	"	z-coordinate of terminal point of streamwise vortex
21-30	D	"	$\Delta y$ shift of terminal point of streamwise vortex

Note: This point also defines the upstream corner of the control point panel if FLAG  $\neq$  2 on Card 14B.

Card 14D2:- Same as Card 14D1, containing the coordinates of the downstream corner of the control point panel if FLAG  $\neq$  2 on Card 14B. If FLAG = 2 on Card 14B, this card contains the coordinates of the upstream corner of the control point panel.

Card 14D3:- If FLAG = 2 on Card 14B, this card contains the coordinates of the downstream corner of the control point panel in the same format as Card 14D1. Omit this card if FLAG  $\neq$  2 in Card 14B1.

Note: Repeat Card 14B and Card Sets 14C and 14D NV times to complete Card Set 14.

Aerodynamic Input Cards:- The configuration panel geometry is transferred to the aerodynamic section of the program by TAPE 11. Additional aerodynamic input cards required are described below.

Card 15:- Case Identification Card. Card 15 contains any desired case identification in Columns 1 - 80.

Card 16:- Iteration Option Card.

<u>Column</u>	<u>Variable</u>	<u>Value</u>	<u>Description</u>
1-10	NIT	arbitrary integer	Maximum number of iterations (15 - 25)
11-20	IEPS	"	Exponent of 10 setting limiting value for residue of iterative solution (-3 or -4 recommended)
21-30	ITYPE	1	Blocked Jacobi iteration procedure
		2	Blocked Gauss-Seidel iteration procedure
		3	Blocked Gauss-Seidel with controlled successive over-relaxation
		4	Blocked Gauss-Seidel with successive over-relaxation

N.B. Option 4 has not been completely checked out, but will be made available at a later date.

Card 17:- Configuration Options.

<u>Column</u>	<u>Variable</u>	<u>Value</u>	<u>Description</u>
1-10	COMPT	0	Forces and moments calculated for complete configuration
		arbitrary integer	Forces and moments calculated on components. Panel indices of each component follow on Card 26
11-20	SECT	0	No wing section forces and moments
		1	Wing section forces and moments calculated. Wing section indices follow on Card 25, panel indices in each section on Card 26, and section reference lengths on Card 29
		2	Forces and moments calculated on subsections. The number of subsections follow on Card 25, the number of panel groups on Card 27, the panel indices in each group on Card 28, and subsection reference lengths on Card 29

Card 18:- Reference Parameters.

<u>Column</u>	<u>Variable</u>	<u>Value</u>	<u>Description</u>
1-10	REFA	arbitrary (fixed point)	Reference data
11-20	REFL	"	Reference chord (MAC)
21-30	XOO	"	Axial distance of leading edge of MAC from origin
31-40	X25	"	Axial distance of quarter chord of MAC from origin

N.B. Default option--all variables set to 1. internally (leave card blank).

Card 19:- Configuration Lift Option.

<u>Column</u>	<u>Variable</u>	<u>Value</u>	<u>Description</u>
1-10	KUT	0	Nonlifting configuration, no vortex-lattice Kutta condition imposed
		1	Lifting configuration, vortex-lattice Kutta condition imposed
		-1	Wing vortex lattice extends through body having same strength as adjacent wing vortex lattice
11-20	NBV	arbitrary integer	Number of body vortices ( $NBV \leq 5$ )
21-30	NV(1)	"	Number of wing vortices associated with body vortex 1
31-40	NV(2)	"	Number of wing vortices associated with body vortex 2
.	.	.	.
.	.	.	.
.	.	.	.
61-70	NV(5)	"	Number of wing vortices associated with body vortex 5

Card 20:- Compressibility Rule Option.

<u>Column</u>	<u>Variable</u>	<u>Value</u>	<u>Description</u>
1-10	KOMPR	1	Gothert Rule 1 selected
		2	Gothert Rule 2 selected
11-20	POINTS	0	One body component case, no off-body points
		1	Flap case, off-body points will be calculated

Card Set 21:- Wind Tunnel Input. The manner in which the wind tunnel is modelled is outlined in the main body of the report.

Card 21A:- Tunnel Length and Relative Location.

<u>Column</u>	<u>Variable</u>	<u>Value</u>	<u>Description</u>
1-10	NHL	arbitrary integer	Number of panels along tunnel half length
11-20	PX	arbitrary (floating point)	x location of tunnel pivot in body co-ordinates
21-30	PZ	"	z location of tunnel pivot in body co-ordinates
31-40	THL	"	tunnel half length <u>in same units as body input</u>

Card Set 21B:- Tunnel Cross-Section.

<u>Column</u>	<u>Variable</u>	<u>Value</u>	<u>Description</u>
1-10	YB	arbitrary (floating point)	y coordinate of point defining an element of tunnel cross-section
11-20	ZB	"	z coordinate of point defining an element of tunnel cross-section
21-25	NBT	arbitrary integer	Number of panels into which line between this point and next point is cut
		-1	Last point defining section

Repeat Card Set 21B as many times as there are straight line elements in tunnel cross-section.

Card Set 22:- Efflux. This permits modelling of efflux or wake flows of known energy level difference.

Card 22A:- Number of Effluxes.

<u>Column</u>	<u>Variable</u>	<u>Value</u>	<u>Description</u>
1-10	NEFF	arbitrary integer ( $<5$ )	Number of separate effluxes

Card 22B:- Efflux Length and Strength.

<u>Column</u>	<u>Variable</u>	<u>Value</u>	<u>Description</u>
1-10	EFL( )	arbitrary (floating point)	Efflux length
11-20	EFGAM( )	"	Efflux strength

Card 22C:- Efflux Cross-Section.

<u>Column</u>	<u>Variable</u>	<u>Value</u>	<u>Description</u>
1-5	NPAN	arbitrary integer  ( $NPAN \leq NEFF < 60$ )	Number of body panel edges defining efflux

Card Set 22D:- Efflux Cross-Section Details.

<u>Column</u>	<u>Variable</u>	<u>Value</u>	<u>Description</u>
1-10	XE(I)	arbitrary (floating point)	ordinates of points defining efflux opening
11-20	YE(I)	"	"
21-30	ZE(I)	"	"

Repeat Card Set 22D NPAN+1 times for each efflux. Repeat Cards 22B and 22C and Card Set 22D for each efflux.

Card 23:- Number of Mach Numbers.

<u>Column</u>	<u>Variable</u>	<u>Value</u>	<u>Description</u>
1-10	NMA	arbitrary integer	Number of Mach numbers following on Card Set 24

Card 24:- Mach Number.

<u>Column</u>	<u>Variable</u>	<u>Value</u>	<u>Description</u>
1-10	MA	arbitrary (floating point)	Mach number

Card 25:- Number of Angles-of-Attack and Yaw.

<u>Column</u>	<u>Variable</u>	<u>Value</u>	<u>Description</u>
1-10	NAL	arbitrary integer	Number of angles-of-attack following on Card Set 26

Card 26:- Angle-of-Attack and Yaw.

<u>Column</u>	<u>Variable</u>	<u>Value</u>	<u>Description</u>
1-10	ALPHA	arbitrary (floating point)	Angle-of-attack in degrees
11-20	BETA	"	Angle-of-yaw in degrees

Card 27:- Number of Sections.

<u>Column</u>	<u>Variable</u>	<u>Value</u>	<u>Description</u>
1-10	IS	arbitrary integer	Number of sections; omit if SECT = 0 on Card 17.

Card 28:- Panel Indices.

<u>Column</u>	<u>Variable</u>	<u>Value</u>	<u>Description</u>
1-10	IA	arbitrary integer	Index of initial panel in section
11-20	IE	"	Index of final panel in section

Card 29:- Number of Panels in Subsections.

<u>Column</u>	<u>Variable</u>	<u>Value</u>	<u>Description</u>
1-10	IREI	arbitrary integer	Number of panels in subsections. Omit if SECT < 2 on Card 17

Card 30:- Subsection Panel Indices.

<u>Column</u>	<u>Variable</u>	<u>Value</u>	<u>Description</u>
1-5	II(1)	arbitrary integer	Panel indices of all panels in subsection; omit if SECT < 2 on Card 17
6-10	II(2)	"	
11-15	II(3)...etc.		

Card 31:- Reference Lengths.

<u>Column</u>	<u>Variable</u>	<u>Value</u>	<u>Description</u>
1-10	DELY	arbitrary integer	Width of section
11-20	REFL	"	Reference length of section
21-30	XLE	"	Moment reference point of section

N.B. Cards 27 - 31 must be repeated for each angle-of-attack or yaw, if section data requested.

Streamline Input Cards:- Each streamline selected is constrained to pass through a chosen panel. This avoids the possibility of the selected streamlines bunching together in the separated flow region.

Card 32:- Case Identification Card. Card 32 contains identification for the streamline calculations.

Card 33:- Streamline Option Card.

<u>Column</u>	<u>Variable</u>	<u>Value</u>	<u>Description</u>
1-10	ENDFILE	-1	Program switches out of WBAERO onto the streamline overlay

Card 34:- Streamline Panel Selection.

<u>Column</u>	<u>Variable</u>	<u>Value</u>	<u>Description</u>
1-5	NLIN	variable	Number of prescribed panels for streamline calculations
6-10	NSP(1)	variable	Panel number for streamline number 1
11-15	NSP(2)	"	Panel number for streamline number 2
16-20	NSP(3)...etc.		

Note: Up to 25 streamlines may be traced if only potential flow is desired. Streamline limit in the boundary layer calculation is 8.

Note: Repeat Card 34 once for every iteration between potential and viscous flow called for by TRMAX on Card 2.

Card Set 35:- This Card Set provides the patch joint overlap information required by the streamline routines.

Card 35A:- Number of Joints to be Input.

<u>Column</u>	<u>Variable</u>	<u>Value</u>	<u>Description</u>
1-5	NJT	arbitrary integer	Number of patch joints following on Card Set 35B

Card Set 35B:- Patch Joint List.

<u>Column</u>	<u>Variable</u>	<u>Value</u>	<u>Description</u>
1-5	JOINT(I,1)	arbitrary integer	Overlapped patch number
6-10	JOINT(I,2)	"	Side number on overlapped patch
11-15	JOINT(I,3)	"	Overlapping patch number
16-20	JOINT(I,4)	"	Side Number on overlapping patch

Repeat Card 35B NJT times (I = 1, NJT)

Card 36:- End of information. 6/7/8/9